

# The Blue Straggler and Main-sequence Binary Population of the Low-Mass Globular Cluster Palomar 13<sup>1</sup>

L. Lee Clark, Eric L. Sandquist

*Astronomy Department, San Diego State University, San Diego, CA 92182*

clark@mintaka.sdsu.edu, erics@mintaka.sdsu.edu

Michael Bolte

*University of California Observatories, Lick Observatory, Board of Studies in Astronomy and Astrophysics, University of California, Santa Cruz, CA 95064*

bolte@ucolick.org

## ABSTRACT

We present high-precision *VI* photometry of stars from the middle of the giant branch to about 5 magnitudes below the main-sequence turnoff in the globular cluster Palomar 13 based on images obtained with the Keck II 10m telescope. We tabulate a complete sample of blue stragglers in the cluster out to about 18 core radii. The blue straggler population is significantly more centrally concentrated than the giant star sample, which is in turn significantly more centrally concentrated than the main-sequence star sample. Palomar 13 has one of the highest specific frequencies of blue stragglers of any known globular cluster, but the specific frequency of blue stragglers in the outskirts of the cluster does not increase as has been seen in denser clusters. We also identify a group of faint blue stragglers (bluer than the turnoff, but having about the same magnitude) that outnumbers the brighter stragglers by more than a factor of 2. The cluster's color-magnitude diagram shows a large excess of stars to the red of the main sequence, indicating that the cluster's binary fraction is at least  $(30 \pm 4)\%$ , which appears to be similar to that of the low-mass cluster E3 but significantly higher than that of the more massive clusters Pal 5 and NGC 288.

*Subject headings:* blue stragglers — binaries: general — globular clusters: individual (Palomar 13, E3, NGC 288, M55, M3, NGC 6752)

---

<sup>1</sup>Based on data obtained at the W.M. Keck Observatory, which is operated as a scientific partnership among the University of California, the California Institute of Technology, and NASA, and was made possible through the generous financial support of the W.M. Keck Foundation

## 1. Introduction

The low-density globular cluster Palomar 13 was discovered on a National Geographic Society-Palomar Observatory Sky Survey photographic plate by Wilson (1955) while searching for Sculptor-type dwarf galaxies within the Local Group. Early color-magnitude studies showed it to be at large galactocentric distance ( $\sim 25$  kpc) and very low luminosity with an integrated absolute magnitude  $M_V \sim -3.4$  (Ciatti, Rosino, & Sussi 1965; Ortolani, Rosino, & Sandage 1985)

Recent studies of Palomar 13 have found indications that the cluster is probably in the late stages of tidal destruction by the Galaxy. Siegel et al. (2001; hereafter SMCT) was the first to measure proper motions of Palomar 13 stars in order to estimate membership probabilities. They found evidence of member stars beyond the cluster’s limiting radius, possibly the result of evaporation or tidal stripping. Côté et al. (2002) presented photometry and radial velocity measurements supporting the idea that the cluster is either in the process of being tidally disrupted, or that its dynamics are dominated by a dark matter halo. Both studies noted a “secondary sequence” beside the single-star fiducial line in the color-magnitude diagram, probably indicating a substantial binary population within the cluster. The existence of such a binary population is consistent with the idea that dynamical processes have led to mass segregation with the preferential loss of low-mass single stars and the retention of more massive binary star systems in the cluster core. However, neither of these studies attempted to characterize the size of the binary population.

Several previous studies (Borissova et al. 1997; Siegel et al. 2001; Côté et al. 2002) have noted the presence of blue straggler stars — in fact, the blue stragglers outnumber the horizontal branch stars in the cluster. It has been recognized for some time that the lower-mass clusters are particularly efficient at producing blue stragglers (Ferraro et al. 1995; Piotto et al. 2004) To date though, *complete* surveys of blue stragglers have been most common in more massive clusters like M3 (Ferraro et al. 1993) and 47 Tuc (Ferraro et al. 2004). The leading explanations for the creation of blue stragglers involve stellar collisions or primordial binary coalescence. Because the dynamics of a cluster will affect the number, period distribution, and evolution of its binary stars, a dynamically mature low-mass, low-density cluster is likely to have a different binary population than will be observed in more massive clusters.

In this paper, we present the results of our photometric study of Palomar 13 examining the effects that the cluster’s dynamics may have had on the stellar population. The greatest obstacle is Palomar 13’s distance. But Palomar 13 provides an excellent opportunity to study blue stragglers: it has little reddening and low field-star contamination (thanks to its high galactic latitude), proper motion membership information is available for stars at

the main sequence turnoff and brighter (SMCT), and the low stellar density makes accurate photometry easy over the cluster’s entire radial extent. On the other hand, an examination of the binary content of the cluster has a few difficulties. While spectra have been obtained for some giant stars Côté et al. (2002), large surveys for radial velocity variations are impractical due to the cluster’s distance. Photometric selection of probable binary stars is more promising, but care must be taken to minimize the small (but nonzero) field star population. Membership information is available from radial velocities and proper motions, but only for stars brighter than about the main sequence turnoff. (In addition, the radial velocity of Pal 13 is quite low, so that there is a relatively small difference between the radial velocities of cluster and field stars (Côté et al. 2002).) To understand the main sequence binary population, we will need to rely on high-quality photometry, both to identify probable binaries and to eliminate as many field stars as possible.

Section 2 gives a brief description of our observations and the data reduction procedures. Section 3 gives a brief discussion of the color-magnitude diagram (CMD). In section 4, we present a thorough study of the blue straggler population within Palomar 13 and compare with other Milky Way globular clusters. In section 5 we place limits on the binary content of the cluster.

## 2. Observations and Data Reduction

We used the Echellette Spectrograph and Imager (ESI, Sheinis et al. 2002) in direct imaging mode on the night of 1999 September 2 to observe Palomar 13 at the 10m Keck II telescope at the Cassegrain focus. ESI in its direct imager mode has a  $2' \times 4'$  field with a  $0''.15 \text{ pix}^{-1}$  scale. The seeing during the run was excellent, with the FWHM of stars ranging between about  $0''.35$  and  $0''.7$ . We collected one 100 s and three 600 s exposures in  $V$ , and one 60 s and three 600 s exposures in  $I$ . In comparison, Côté et al. (2002) only had two exposures in each filter (10 and 300 s in  $V$ , and 6 and 180 s in  $I$ ). The seeing for their frames ranged from  $0''.7$  to  $0''.8$ . Each of these factors contributed to a noticeable improvement in the photometric scatter on the lower main sequence in our photometry compared to theirs.

The Keck cluster images were bias-subtracted and flat-fielded using IRAF<sup>2</sup>. The photometric measurements were made using point-spread function fitting in the programs DAOPHOT II and ALLSTAR (Stetson 1993). All of the frames were reduced once, and object-subtracted

---

<sup>2</sup>IRAF (Image Reduction and Analysis Facility) is distributed by the National Optical Astronomy Observatories, which are operated by the Association of Universities for Research in Astronomy, Inc., under contract with the National Science Foundation.

frames from ALLSTAR were examined to recover additional stars. A new master list of stars was then derived from those objects that were found in all three 600 s  $I$ -band exposures. This list was then merged with the list of objects found in all three 600 s  $V$ -band exposures (which did not go as faint as the  $I$ -band frames), and the combined list was used in final runs of ALLSTAR on the long exposure frames. The final star list was made by finding stars that were detected in both filter bands.

We calibrated our photometry to that of Côté et al. (2002), whose dataset had a comparable faint limit to ours, and who were able to observe Landolt (1992) standard fields interspersed with their cluster field. We chose stars with  $V < 23$  and  $(V - I) < 1.05$  for the calibration. Although our absolute photometry is not independent of theirs, our *relative* photometry is an improvement over that of Côté et al. (2002).

The equations used in the photometric transformations are:

$$v = V + a_0 + a_1(V - I) + a_2(V - I)^2 \quad (1)$$

$$i = I + b_0 + b_1(V - I) \quad (2)$$

where  $v$  and  $i$  are instrumental magnitudes, and  $V$  and  $I$  are standard magnitudes. The color transformation coefficients were  $a_1 = 0.100 \pm 0.040$ ,  $a_2 = -0.037 \pm 0.029$  and  $b_1 = 0.107 \pm 0.015$ . A comparison of our calibrated photometry with that of Côté et al. (2002) is shown in Fig. 1, along with median residuals. Our photometry is very accurately placed on the same system as that of Côté et al. (2002), with the exception of a slight ( $\sim 0.02 - 0.03$  mag) systematic trend in  $I$  for stars on the giant branch. Côté et al. (2002) compared their photometry with that of previous studies, finding good agreement with that of Siegel et al. (2001), but finding significant offsets and trends with magnitude and color compared to earlier photometric studies (Ortolani et al. 1985; Borissova et al. 1997).

### 3. The Color-Magnitude Diagram (CMD)

Fig. 2 shows the CMD of the 478 stars detected in both filters with  $18.5 \lesssim V \lesssim 26.5$ . The main source of contamination in the CMD for this cluster was background galaxies. We therefore employed a cut on the image sharpness provided by ALLSTAR for each object:  $-0.5 < \text{SHARP} < 0.5$ . This cut only affected objects fainter than the cluster turnoff ( $V_{TO} \approx 21.15 \pm 0.10$ ). Bright cluster stars were saturated in all of our Keck images. The photometric precision for main-sequence stars is relatively high, as can be seen by comparing the lower main sequence in Fig. 2 and Fig. 4 of Côté et al. (2002). In Fig. 3, we present plots comparing formal measurement errors in  $V$  and  $I$  for the measurements from this study and that of Côté et al. (2002). The reduction in the photometric scatter allows us to clearly

see a substantial population of stars to the red of the single-star main sequence. This group of stars is interpreted as a binary star population as will be discussed further in section 5.

Our photometry sample is smaller than that of Côté et al. (2002) due to smaller field size. Because Côté et al. (2002) discussed the main-sequence luminosity function for Palomar 13, we will not present a new analysis here. Regardless, the luminosity function is nearly flat with magnitude, a fact which can almost be seen by eye in the CMD. This is cited as evidence of the effectiveness of mass segregation and the evaporation of low-mass stars. Similar flat luminosity functions have been measured for other more massive clusters like Palomar 5 (Grillmair & Smith 2001; Odenkirchen et al. 2002) and NGC 6752 Rubenstein & Bailyn (1999).

## 4. Straggler Stars and Bright Binary Systems

### 4.1. Background

The leading explanations for blue straggler star formation involve the creation of a star more massive than the turnoff mass after the epoch of star formation in the cluster. Primordial binaries evolving into contact are the leading candidates for forming field blue stragglers — spectroscopic binaries with low eccentricity found among halo blue stragglers imply that mass transfer is important (Carney et al. 2001). In the denser environments of globular clusters, binary star evolution may still play an important role, but stellar collisions (involving single or binary stars) are also likely to form some fraction of the population. Efforts are now being made to identify the relative roles of these different formation mechanisms. For example, the specific frequency of blue stragglers as a function of radius has a minimum at intermediate radii in more massive clusters like M3 (Ferraro et al. 1993), M55 (Zaggia, Piotto, & Capaccioli 1997), and 47 Tuc (Ferraro et al. 2004). The core population of stragglers may be produced in collisions, while the envelope population may be produced largely by primordial binary stars whose orbits in the cluster have not changed significantly since the cluster’s formation (Mapelli et al. 2004). Alternately, binaries that interact within the core of the cluster can create blue stragglers with varying amounts of recoil, so that the ones given little recoil quickly relax back to the cluster core, while those given larger recoil end up spend mosting of their lives in the outskirts of the cluster (Sigurdsson, Davies, & Bolte 1994).

The continuing interest in blue stragglers is partly because they may provide a means of gauging the recent dynamical history of a cluster. Binary star systems are an important source of kinetic energy that can be tapped by cluster stars during strong gravitational

interactions, which can in turn have a significant effect on the evolution of the cluster’s structure. The radial distributions of blue stragglers may be revealing information about the timescale on which dynamical friction modifies the stellar orbits (Mapelli et al. 2004). CMD information may also lead to an understanding of blue straggler formation (Sills & Bailyn 1999), which may be connected to the dynamical evolution of the cluster — for example, 47 Tuc may have ceased vigorous formation of blue stragglers several Gyr ago (Sills et al. 2000).

There are several reasons for focusing attention on low-density clusters like Palomar 13. Observationally, it is a considerably easier task to obtain a complete sample of good blue straggler candidates in low-density clusters than in higher-density ones because of the greatly reduced probability of image blending. Studies by Ferraro et al. (1995) and Piotto et al. (2004) have indicated that low-density globular clusters often have some of the highest specific frequencies of blue stragglers. In low density systems like Palomar 13, the expectation is that primordial binary stars are most important in blue straggler formation, although theoretical studies of open clusters like M67 indicate that binary-binary interactions may still play an important (or even dominant) role in producing stragglers (Hurley et al. 2001). There is good evidence that at least three blue stragglers in M67 were formed via collisions involving more than two stars: S977 (Leonard 1996), S 1082 (van den Berg et al. 2001; Sandquist et al. 2003), and S 1284 (based on the eccentricity of the short period orbit of the blue straggler’s companion; Milone & Latham 1992). Other stragglers in long-period eccentric binaries might also be the result of collisions involving a binary system. For clusters that are on the verge of tidal destruction, there may be a competition between decreasing stellar density (due to the evaporation of low-mass stars) and increasing binary fraction (resulting from mass segregation).

## 4.2. Palomar 13 Blue Stragglers

As can be seen in the CMD (Fig. 4), Palomar 13 has a healthy population of blue straggler stars, even outnumbering the horizontal branch stars in the cluster. Blue stragglers are typically identified as stars that are significantly brighter and bluer than the cluster’s turnoff ( $V < 21.2$ ). The region populated by stragglers is roughly bounded on the blue side by a zero-age main sequence of the appropriate composition. The reason for this is thought to be that blue stragglers are rejuvenated stars with higher central hydrogen content than single stars at the cluster turnoff. (This is independent of the actual physical mechanism that causes this increase in central hydrogen abundance.) In the open cluster M67 (Sandquist & Shetrone 2003), there is a large population of stars with colors between the fiducial line

of the cluster and the zero-age main sequence, but with brightnesses placing them at or fainter than the cluster turnoff. These stars are more difficult to identify in CMDs than canonical blue stragglers if the photometry is poor, but there is every reason to identify them as “rejuvenated” blue stragglers. As a result, we have attempted to identify *all* bright cluster members that have photometry placing them significantly to the blue of the single-star sequence. This includes three stars about 0.6 mag fainter than the turnoff that were identified by the significance of their deviation from the cluster fiducial line.

“Yellow” or “red stragglers” are stars with colors between that of the turnoff and the red giant branch, but brighter than the subgiant branch. Such stars have been identified in open and globular star clusters — these stars may be former blue straggler stars that are now evolving toward the giant branch, binary star systems or blends of unassociated stars (most likely for stars within 0.75 mag of the subgiant branch), or something more exotic. In a sparse globular cluster like Pal 13, blends of unassociated stars are fairly unlikely. For these reasons, we have also tried to identify stars that could fall in this class.

Table 1 lists all of the stars we identified (a total of 32) as blue or red straggler star (BSS or RSS) candidates in Palomar 13 based on position in the CMD and proper motions (Fig. 4). We also cross-identified our list with the photometry of Côté et al. (2002) and Siegel et al. (2001). Column 1 of the table gives the ID number from this study, column 2 the ID number from Siegel et al. (2001), column 3 the ID number from Côté et al. (2002), columns 4 and 5 the position relative to the cluster center in arcsec, columns 5-8 the  $V$  magnitude and  $(V - I)$ ,  $(B - V)$ , and  $(U - V)$  colors from the different datasets, and column 9 the Siegel et al. membership probability. Star positions were measured relative to the coordinates of the cluster center ( $\alpha = 23^{\text{h}}06^{\text{m}}44^{\text{s}}.8$ ,  $\delta = 12^{\circ}46'18''$ ; epoch 2000.0) determined by Siegel et al. (2001). Proper motions from Siegel et al. (2001) were used to eliminate high-probability field stars when possible. Two candidate BSS stars (IDs 67 and 117) are probable nonmembers ( $0 < P_{\mu} < 0.4$ ), although one is at the faint end of the SMCT sample. 10 candidates have questionable membership ( $0.4 < P_{\mu} < 0.8$ ), and there is no proper motion information on another five of our candidates. Since the field of Côté et al. (2002) extended beyond our observed field, we used their photometry to identify 5 additional candidates (although three of these appear to be field stars). Several of the stars in our list fall close enough to the subgiant branch that there is a substantial probability that they are detached binary systems — these stars are identified in the table, and were noted by SMCT as an apparent sequence of stars parallel to the subgiant branch.

Borrisova et al. (1997) and Siegel et al. (2001) each identified seven BSS candidates. However, our smaller measurement errors for stars near the cluster turnoff allow us to identify candidates that are closer to the main-sequence turnoff in the CMD, and our better image

resolution allowed us to locate BSS candidates closer to the cluster core. One of the BSS candidates (BSS 4; SMCT ID 428) that was originally identified by Borissova et al. (1997) is not included here because it clearly falls within the cluster main-sequence turnoff band in our photometry and has a low membership probability ( $P = 0.23$ ). The following subsections will provide analysis of our BSS population and comparison of Palomar 13’s population with other clusters.

The brightest straggler (ID 2) deserves some comment. From proper motions, the star has a moderate probability of membership, but Blecha et al. (2004) made two radial velocity measurements for the star (25.85 and 25.67 km s<sup>-1</sup>) placing it quite near the cluster mean ( $24.1 \pm 0.5$  km s<sup>-1</sup>). Given that it is the brightest blue straggler in the cluster, its red color is surprising. A blend of a bluer blue straggler with a faint red giant can probably be ruled out since the star’s  $U - V$  color is consistent with colors using other filter combinations. Models of stellar collisions (e.g. Sills & Bailyn 1999) generally predict that the most massive blue stragglers will tend to be among the bluest, primarily as a result of the relationship between effective temperature and mass for main sequence stars. Spectroscopic measurement of the star’s surface gravity might help verify whether it is an evolved blue straggler or not.

At the risk of overanalyzing this relatively small population of stragglers, we note a couple of features of the CMD distribution. The color distribution for the seven brightest BSS shows no tendency for the stragglers to cluster toward the zero-age main sequence. In fact, these stragglers are spread almost evenly from near the zero-age main sequence to the turnoff color. This type of color distribution is seen in many other clusters, and is not predicted by models of stellar collisions (e.g., Sills & Bailyn 1999). In addition, there is a gap of over 0.5 mag between the bright blue stragglers and the 17 straggler candidates fainter than the subgiant branch.

### 4.3. Radial Distribution

In an effort to learn more about the effects of cluster dynamics on the BSS population, we compared the cumulative radial distribution of the BSS to the populations of giant branch ( $V < V_{TO}$ ) and main sequence stars. In order to cover the widest range of radii possible, we combined our data with those of Côté et al. (2002). Field stars were eliminated using proper motion (Siegel et al. 2001) and radial velocity (Côté et al. 2002) information for the giant stars, and CMD location for the main-sequence stars. After these cuts, there were 83 stars in the giant sample and 543 stars in the main sequence sample. Typically the straggler population is compared to brighter populations (for example, horizontal branch stars), but because these stars are so rare in Palomar 13, we were forced to resort to fainter



populations. Kolmogorov-Smirnov (K-S) probability tests were used to test the hypothesis that the populations were drawn from the same parent population. The cumulative radial distributions are shown in Fig. 5. The results of the K-S tests are given in Table 2, including the absolute deviation  $D$  and the probability  $P$  that the two samples were drawn from the same distribution.

The central concentration of the blue stragglers relative to the cluster light has been noted before by Siegel et al. (2001). However, our results show that there are *significant* differences between all three samples, with the BSS distribution being the most centrally concentrated, and the MS sample being the least concentrated. The probability that any one of the populations was drawn from the same distribution as another is less than 0.06%. Just four of the selected BSS are found outside a radius of  $42''$  ( $\sim 3r_c$  according to Côté et al. (2002)).

Because the number of blue stragglers is relatively small, we now examine what effect the exclusion of subsets of stragglers has on the results of the K-S tests. The elimination of the six BSS candidates redder than the turnoff color (stars which have a considerably higher probability of being detached binaries) has a minor effect on our conclusions: there is still a probability of less than 0.1% that the BSS and giant samples come from the same distribution. We have also looked at the distributions of the brightest 7 and faintest 19 of the stragglers and find that their radial distributions are indistinguishable. There is a 12% chance that the bright BSS sample was drawn from the same distribution as the giants, although this is primarily due to the small size of the sample and the single bright BSS (BSS 7 from SMCT) at  $185''$  from the cluster center. The faint sample has just a 0.4% chance of being drawn from the same distribution as the giants.

The cumulative radial distributions should make it clear that there is a large increase in the relative frequency of blue stragglers going toward the core of the cluster. Recent studies of much more massive globular clusters (Ferraro et al. 1993; Zaggia et al. 1997; Ferraro et al. 2004) have indicated that the blue straggler frequency decreases at intermediate radii before rising again at large distances from the center. Because the typical normalizing populations (HB or bright RGB stars) are small in number in Palomar 13, we have chosen to normalize the blue straggler frequency to the fraction of the integrated flux from all other detected cluster stars (see Fig. 6).

We also plot the specific frequency defined by Ferraro et al. (1993). We find that the specific frequency of blue stragglers in the core of Palomar 13 is comparable to that of much denser clusters like M3 (Ferraro et al. 1993) and 47 Tuc (Ferraro et al. 2004), but we see no signs of an upturn in the specific frequency of stragglers at large radii seen in these denser clusters. In M3 and 47 Tuc, this upturn occurs at  $\sim 10r_c$ . In the low-concentration ( $c = 0.8$ )

cluster M55, the upturn occurs at  $r \simeq 2r_c$  (Zaggia et al. 1997). Given  $r_c = 14''$  (Côté et al. 2002), Palomar 13 has been surveyed out to nearly  $18r_c$ . The lack of an upturn probably cannot be ascribed to small number statistics: the specific frequency would need to be almost 10 times higher than measured to be consistent with the denser clusters. However, there is a possibility that the relative frequency of stragglers could increase at much larger radii than surveyed here given that the best fitting King-Michie model has a tidal radius  $r_t = 26' \pm 4'$  (Côté et al. 2002). From the wider-field ( $7' \times 14'$ ) CFHT photometry of Côté et al. (2002) (their Fig. 6), there is only one blue straggler candidate outside the field discussed in this paper, and it is at more than twice the distance from cluster center as any other straggler and has no membership information at present. While this result should be tested in surveys of other low-mass globular clusters, the blue straggler distribution may be fundamentally different than those of more massive clusters.

#### 4.4. Blue Straggler Population Comparison

To put the Palomar 13 blue straggler population in perspective, we would like to compare the global BSS population to that of other globular clusters. Recently Piotto et al. (2004) published results for frequencies of blue stragglers relative to HB and RGB stars for 56 globular clusters. Palomar 13 has much lower values for integrated luminosity and central luminosity density than any of the clusters in the Piotto et al. sample.

Piotto et al. found a significant anticorrelation between the specific frequency  $F_{BSS}^{HB} = N_{BSS}/N_{HB}$  and integrated luminosity  $M_V$ , a weaker anticorrelation with central density  $\log \rho_0$ , and no significant trend with expected collision rate  $\log \Gamma_*$ . From the globular cluster catalog of Harris (1996), Palomar 13 has  $M_V = -3.74$ ,  $\log \rho_0 = 0.40$  ( $\rho_0$  in  $L_\odot \text{ pc}^{-3}$ ), and  $\log \Gamma_* = -16.25$  (calculated according to the procedure given in Piotto et al.). There are five HB stars (four RR Lyrae stars, and one nonvariable) known in the cluster within the area covered by our photometry and that of Côté et al. (2002). The blue straggler samples in Piotto et al. (2004) were not selected using uniform criteria for all clusters (F. De Angeli, priv. comm.), so we discuss two selections. Restricting our blue straggler sample to those having  $V < 20.4$  (the level of the base of the giant branch) and  $(V - I) < 0.65$ , we are left with 7 stars, giving  $F_{BSS}^{HB} = 1.4 \pm 0.8$  (using Poisson error estimates). Only two clusters (NGC 6717 and NGC 6838) in the Piotto et al. study have higher values. These two clusters were the faintest ones included in the Piotto et al. study, though they have central densities that are more than two orders of magnitude higher. If we accept all of the blue straggler candidates that are bluer than the turnoff, we have  $N_{BSS} = 26$  and  $F_{BSS}^{HB} = 5.2 \pm 2.5$ , which is higher than any cluster value in the Piotto et al. sample.

Piotto et al. also examined the blue straggler population relative to the amount of flux sampled, and once again they found a significant anticorrelation with the absolute magnitude of the cluster. When the Côté et al. (2002) dataset is combined with ours, nearly the entire flux from the cluster is sampled, which gives us  $\log N_S(BSS) = -0.65$  or  $-0.08$  depending on whether the more restrictive sample of blue stragglers is used. (For comparison,  $\log N_S(HB) = -0.80$ .) For the restricted sample, the  $\log N_S(BSS)$  value places Palomar 13 among the clusters with the highest values, but for the total sample, Palomar 13 has a value second only to NGC 6838, a cluster that is more than 5 times brighter ( $M_V = -5.60$ ; Harris 1996).

This study makes Palomar 13 the faintest globular cluster with a thoroughly studied BSS population, covering from the cluster center out to nearly 18 core radii. In combination with the results from Piotto et al. (2004), Palomar 13 provides additional evidence that the production of blue stragglers relative to the cluster HB stars or the cluster light may plateau for clusters with  $M_V \gtrsim -6$  (see Fig. 1 of Piotto et al. (2004)). On the other hand, because Palomar 13 appears to be a cluster in the throes of tidal disruption by the Galaxy, it is possible that the binary fraction in the cluster may have been artificially elevated during mass segregation, affecting the size of the straggler population.

## 5. Binary Fraction

A characterization of the binary population in Palomar 13 can provide important information about the dynamical environment and history of the cluster. As a cluster undergoes mass segregation as a result of internal dynamics, and loses stars due to its tidal interaction with the Galaxy, the fraction of cluster stars in multiple star systems will increase. Siegel et al. (2001) noticed an apparent double subgiant branch that could be due to the presence of near equal-mass binary stars. Their photometry only reached the main sequence turnoff, however. Côté et al. (2002) noticed evidence for a “second sequence” running parallel to the cluster’s main sequence in its CMD, but did not characterize it. As can be seen in Fig. 7, the sequence is better defined in our dataset.

Probably the most direct means of estimating the global binary fraction is to characterize the population of cluster stars falling to the red of the single-star main sequence (Rubenstein & Bailyn 1997; Bolte 1992; Romani & Weinberg 1991), where binary stars and optical blends of cluster stars fall in the CMD. We have chosen to use a method similar to the one outlined by Bolte (1992) that provides an estimate of the fraction of stars in a cluster that are in binary systems, independent of assumptions about binary star properties like the mass ratio distribution.

Our analysis only makes use of photometry from this study since the sample of Côté et al. (2002) had larger amounts of photometric scatter and field star contamination. The main sequence stars in the CMD were first used to create a fiducial line for the cluster (Fig. 7). This was accomplished by iteratively fitting the main sequence sample with a polynomial and rejecting stars with photometry that placed them more than a threshold number of  $\sigma$  (from the photometric errors) away from the fit. The threshold value was initially chosen to be large ( $10\sigma$ ) and was then reduced. The final fit used a fifth-order polynomial and a  $2.5\sigma$  rejection cut. Because the stars toward the blue side of the main sequence are most common, the fit naturally migrates toward that edge (where the single-star main sequence is expected to be). This method also has the advantage of requiring minimal human intervention and no judgement on which stars to select for the fit.

We then determined the color deviation  $\Delta(V - I)$  between the color of each star and the color of the main sequence fit. Thus, single stars will be distributed about  $\Delta(V - I) = 0$ , while main sequence binary stars will be distributed to the red ( $\Delta(V - I) > 0$ ). The middle panel of Fig. 7 shows a line corresponding to the expected positions of equal-mass binary systems — there is a clear excess of stars found to the red of the main sequence as compared to the blue side. Fig. 8 plots the number of  $\sigma_{V-I}$  of deviation from the main sequence fit versus magnitude, showing that the stars to the red have significant deviations.

The derivation of a binary fraction from this distribution is complicated by the small number of stars in the cluster and by changes in the slope of the main sequence as a function of magnitude. Therefore, we opted to divide the color deviations for each star by the *expected* color deviation for an equal-mass binary system  $\Delta(V - I)_{bin}$  to get the quantity  $R_{VI} = \Delta(V - I)/\Delta(V - I)_{bin}$ . This has the benefits that there is a monotonic relationship between  $R_{VI}$  and  $\Delta V$  (the difference between the magnitude of the primary and the magnitude of the binary system), and  $R_{VI}$  is very nearly constant for a binary system of given  $\Delta V$  along the entire main sequence (see Fig. 9). The result of this procedure is shown in the right panel of Fig. 7. In this way, stars measured over most of the magnitude range of the observed main sequence can be compared. This procedure amplifies measurement errors on the upper main sequence (because the main sequence is steeper, and  $\Delta(V - I)_{bin}$  is smaller). However, the photometric errors for these stars are usually much smaller than for stars on the lower main sequence, so that this amplification is a minor effect.

The distribution of stars in  $R_{VI} = \Delta(V - I)/\Delta(V - I)_{bin}$  was then histogrammed for  $21.2 < V < 24.2$  (eliminating faint stars with the largest photometric uncertainties and stars above the level of the turnoff). The estimation of the binary fraction is dependent on the assumption that the single star population of the cluster falls in a Gaussian distribution centered around  $R_{VI} = 0$ . We estimated the size of the dominant population of single stars

and binary stars with extreme luminosity ratios ( $R_{VI} \approx 0$ ) with two different procedures.

Our first method employed artificial star tests to predict the  $R_{VI}$  distribution for a set of single stars covering a range of magnitudes. This distribution will differ from Gaussian because fainter stars have larger measurement errors and will therefore cover a larger range in  $R_{VI}$ . We conducted 30 artificial star runs on our images, placing approximately 700 artificial main sequence stars in the field for each run. The CMDs of the input and recovered artificial stars are shown in Fig. 10. We then determined the width of the distribution in  $R_{VI}$  for all stars in 0.5 mag bins by fitting a Gaussian to stars within  $1.5\sigma$  of  $R_{VI} = 0$ . The predicted single-star distribution for real stars was then computed by summing Gaussians of unit area (one Gaussian for each star within  $2\sigma$  of  $R_{VI} = 0$ ) having FWHMs corresponding to that of the artificial star distribution for the same magnitude bin. After the predicted distribution was subtracted from the distribution of real stars, the red ( $R_{VI} > 0$ ) and blue sides of the residual distribution were integrated. If the residuals on the blue side are part of a symmetric distribution of stars with large photometric errors, then an equal contribution must be subtracted from the red side in order to compute the binary fraction.

Using this method on the distribution of real stars, we found 121.7 stars in the central peak, and once this contribution was subtracted, there were 83.4 stars left on the red side of the peak, and 12.0 stars on the blue side. (9 stars on the blue side were blue stragglers, and were not considered.) This results in a net contribution of 71.4 stars from the red side, which produces a binary fraction of  $0.31 \pm 0.04$  (with the uncertainty computed using Poisson statistics).

As a check, we investigated whether unresolved blends of unassociated single stars could produce the binary fraction measured above. We determined the binary fraction that would be determined from all artificial stars placed within  $1'$  of the cluster center. The result of these artificial star tests is shown in 11. For the 4738 artificial stars falling in the magnitude range analyzed for the binary fraction, we found 107 net stars on the blue side and 169 net stars on the red side of the predicted single-star distribution, giving a binary fraction  $0.013 \pm 0.002$ . Although the artificial star experiments demonstrate that blends contribute to the binary fraction measurement even in a cluster this sparse, blends are far too unlikely to explain a binary fraction as high as 30%.

For the second method of determining the binary fraction, we simply fit a Gaussian distribution to the central peak of the real star distribution ( $|R_{VI}| < 0.3$ ), returning a mean of 0.0052 and  $\sigma = 0.144$  (see Fig. 12). After the Gaussian was subtracted, the red and blue sides were integrated out to  $R_{VI} = 1.4$ . We integrated beyond  $R_{VI} = 1$  on the red side because errors in the photometry of nearly equal-mass binary systems could cause them to have  $R_{VI} > 1$ . The integrations of the blue and red sides returned 12.4 and 80.9 stars

respectively. (Once again, blue stragglers were not considered.) If we again assume that the distribution on the blue side is part of a symmetric distribution of stars with large photometric errors, we are left with a net contribution of 68.5 stars from the red side. We measured 123.7 stars in the central peak. Adding in the contribution from the stars on the blue side and an equal contribution from stars on the red side yields a total single-star content of 148.5 stars, which results in a binary fraction of  $0.32 \pm 0.04$ . The results from the two methods described above matched well in part because we restricted ourselves to stars significantly brighter than the faint limit of the survey, so that photometric errors did not end up broadening the total star distribution excessively.

In the deep exposures we discussed here, we also need to consider contaminating objects like background galaxies and field stars. The primary source of contamination for the upper main sequence seems to be galaxies. Our use of a cut on image SHARP-ness eliminated a large fraction of the objects red of the expected position of the equal-mass binary sequence and blue of the single-star main sequence. Based on this, we do not regard galaxies as a likely source of contamination for the upper main sequence used in the binary fraction analysis. Field star contamination could artificially boost the measured binary fraction if a significant number of stars fall between the single-star main sequence and the equal-mass binary sequence. The blue edge of the field star population falls near the main sequence of Pal 13 (for example, compare the  $BV$  data of the north Galactic pole in Fig. 2a of Reid & Majewski (1993) with Fig. 4 of Côté et al. (2002)). However, the field star distribution extends far to the red. As a result, the very small number of stars redward of the equal-mass binary sequence can be taken as evidence that the field star contribution is minimal.

The general technique was first applied by Bolte (1992) to NGC 288, giving  $f_b \sim 0.15$ . Comparing Bolte’s Fig. 11 with our Fig. 12, the binary fraction in Palomar 13 is noticeably larger than in NGC 288. Veronesi et al. (1996) examined the loose globular cluster E3 using a method roughly equivalent to ours and found  $f_b = 0.29 \pm 0.09$ , which is quite similar to the value we derive for Palomar 13. On the other hand, Koch et al. (2004) found  $f_b = 0.09 \pm 0.01$  for the core ( $r < r_c$ ) of the cluster Pal 5, with comparable values out to 3 core radii. Of these clusters, E3 and Pal 13 have similar integrated magnitudes ( $M_{V_i} = -2.77$  and  $-3.74$ , respectively; Harris 1996), while Pal 5 ( $M_{V_i} = -4.77$ ; Odenkirchen et al. (2002)) and NGC 288 ( $M_{V_i} = -6.74$ ; Harris 1996) are considerably brighter. The idea that fainter clusters have higher binary fractions should be tested with additional studies of clusters in this range.

Because there is not a noticeable residual of stars with  $0 < R_{VI} < 0.3$ , we can consider these measurements to be the binary fraction for systems with  $R_{VI} > 0.3$  ( $R_{VI} = 0.3$  roughly corresponds to  $\Delta V = 0.25$ , which means the primary contributes about 80% of the system light.) The numbers we quote above are rough *lower limits* to the *total* percentage

of unresolved binary systems since systems with small mass ratios would tend to be counted as single stars. An estimation of the total binary fraction requires assumptions about the distribution of mass ratios in binary systems  $F(q)$  and extensive artificial star tests. Such studies have been carried out for the globular clusters NGC 288 ( $0.08 \lesssim f_b \lesssim 0.38$  within 1.6 core radii, and  $f_b < 0.1$  outside that; Bellazzini et al. 2002) and NGC 6752 ( $0.15 \lesssim f_b \lesssim 0.38$  for the inner core radius,  $f_b \leq 0.16$  for the outer core radius; Rubenstein & Bailyn 1997). These two clusters have central densities that differ by a factor of  $\sim 1300$  (Harris 1996), and probably also have very different dynamical histories. Ferraro et al. (2003a) find evidence that the surface brightness profile of NGC 6752 is best fitted by a *double* King-model profile, concluding that it is in a post-core-collapse phase. NGC 288 has probably had a history similar to that of Palomar 13, since there are indications of an extratidal tail implying significant mass loss from the cluster (Forestell et al. 2001). However, in their detailed analysis of NGC 288, Bellazzini et al. found that although they achieved compatibility between their numerical simulations and observations for  $0.05 \leq f_b \leq 0.30$ , the highest degree of compatibility was for  $0.10 \leq f_b \leq 0.20$  (in agreement with Bolte’s earlier analysis). We conclude that it is very likely that Palomar 13 has a higher binary fraction than NGC 288, and is almost certainly in a more advanced stage in its tidal destruction.

We checked to see whether the identified binary population ( $R_{VI} > 0.3$ ) followed the same radial distribution as the rest of the main sequence stars. Because our dataset was the only one appropriate to carry out this analysis, the cumulative radial distributions shown in Fig. 13 completely cover only the innermost 75'' of the cluster. A K-S test indicates that there is a 55% chance that the two samples come from the same distribution. There is a similar chance (51%) that the subgiant and red giant sample comes from the same distribution as the combined single-star and binary sequences. This analysis is limited by the radial coverage of the cluster in our images and small-number statistics. However, Koch et al. (2004) found in their study of Pal 5 that the total binary and single star populations had similar radial distributions, but brighter photometric binaries appeared to be more centrally concentrated than fainter ones. If this also holds for Pal 13, it would help to hide differences between the binary and single star populations. Deeper and wider-field images will be needed to determine whether the binary star radial distribution deviates from that of the single stars in any substantial way.

## 6. Conclusions

In this paper we have presented high-precision photometry for stars in Palomar 13 between the horizontal branch and over 3 magnitudes below the main sequence turnoff. The

photometry has allowed us to simultaneously compile a complete sample of blue stragglers and characterize the overall binary fraction for this low-mass globular cluster. We find that the specific frequency of blue stragglers in this cluster is one of the highest known. The cumulative radial distributions of stragglers, subgiant and giant stars, and main sequence stars each show highly significant differences. The cluster binary fraction is quite high ( $f_b \gtrsim 0.30 \pm 0.04$ ), similar to another low-mass cluster (E3).

Palomar 13 is now one of the few clusters in which the blue straggler population has been almost completely surveyed *and* the binary fraction has been constrained. The high binary fraction (probably the result of mass segregation and tidal evaporation) could be directly involved in creating the high specific frequency of blue stragglers seen in the cluster. Davies, Piotto, & De Angeli (2004) present a hypothesis that blue straggler populations are produced in collisions (a mechanism that dominates if  $M_V \lesssim -8.8$ ) or primordial binary systems. In their scenario, none of Palomar 13’s stragglers would have resulted from collisions. Palomar 13 would also have started with a larger binary fraction because a larger proportion of its binary systems would have avoided breakup in interactions with other stars. Davies et al. calculate that the binary fraction would scale linearly with  $\log M_{tot}$  if the initial distribution of binary separations is uniform in  $\log a$ , where  $a$  is the average separation.

The situation may not be this simple if Palomar 5 is any indication: Odenkirchen et al. (2002) find a binary fraction of only 10%, which is lower than those of both Pal 13 and NGC 288. In addition, the Davies et al. scenario assumes that globular clusters have essentially evolved in isolation. The blue straggler population of the cluster might be expected to show qualitative differences depending on its dynamical history — whether it began life as a very low-mass globular cluster or if it was initially more massive and was heavily affected by evaporation of its lower mass stars. Earlier studies (Siegel et al. 2001; Côté et al. 2002) present evidence that evaporation probably played a major role. If true, then the effects (if any) would show up in the faint population of stragglers because their lifetimes are a much larger fraction of the lifetime of the cluster. If primordial binary stars are largely retained by the cluster during evaporation, then the blue straggler population of the cluster should be the equivalent of that of a more massive cluster. A cluster that had low mass from the beginning would have a smaller straggler population overall (although this would be partially compensated for by a larger binary fraction).

On the other hand, the horizontal branch population in Palomar 13 is roughly consistent with that of a cluster of its *current* mass. Piotto et al. (2004) show that the number of horizontal branch stars per unit absolute visual flux is very nearly constant over 4.5 mag in  $M_V$ . If anything, Palomar 13 has fewer HB stars than expected for its luminosity. In conjunction with the cumulative radial distributions (discussed in this paper) and the flatness



of the main sequence luminosity function (Côté et al. 2002), this indicates that *evaporation is affecting single stars throughout the main sequence and giant branch of this cluster*. These (admittedly simple) arguments imply that tidal effects on a cluster may constitute a second-order influence on the size of a cluster blue straggler population.

The authors wish to thank P. Côté and M. Siegel for the generous use of their datasets on the cluster, and the anonymous referee for comments that helped improve the manuscript. L.L.C. would like to thank L. M. Hicks, L. Layton, and N. Fekadu. E.L.S. also wishes to thank F. De Angeli for helpful conversations. This research was supported by the National Science Foundation under grant AST 00-98696.

## REFERENCES

- Abell, G. O. 1955, *PASP*, 67, 258
- Bellazzini, M., Fusi Pecci, F., Messineo, M., Monaco, L., & Rood, R. T. 2002, *AJ*, 123, 1509
- Blecha, A., Meylan, G., North, P., & Royer, F. 2004, *A&A*, in press
- Bolte, M. 1992, *ApJS*, 82, 145
- Borissova, J., Markov, H., & Spassova, N. 1997, *A&AS*, 121, 499 (BMS)
- Carney, B. W., Latham, D. W., Laird, J. B., Grant, C. E., & Morse, J. A. 2001, *AJ*, 122, 3419
- Côté, P., Djorgovski, S. G., Meylan, G., Castro, S., & McCarthy, J. K. 2002, *ApJ*, 574, 782
- Davies, M. B., Piotto, G., & de Angeli, F. 2004, *MNRAS*, 349, 129
- Ferraro, F. R., Beccari, G., Rood, R. T., Bellazzini, M., Sills, A., & Sabbi, E. 2004, *ApJ*, 603, 127
- Ferraro, F. R., Fusi Pecci, F., Cacciari, C., Corsi, C., Buonanno, R., Fahlman, G. G., & Richer, H. B. 1993, *AJ*, 106, 2324
- Ferraro, F. R., Fusi Pecci, F., & Bellazzini, M. 1995 *A&A*, 294, 80
- Ferraro, F. R., Possenti, A., Sabbi, E., Lagani, P., Rood, R. T., D’Amico, N., & Origlia, L. 2003a, *ApJ*, 595, 179
- Ferraro, F. R., Sills, A., Rood, R. T., Paltrinieri, B., & Buonanno, R. 2003, *ApJ*, 588, 464

- Forestell, A. D., Majewski, S. R., Westfall, K. B., Patterson, R. J., & Kunkel, W. E. 2001, *BAAS*, 33, 1385
- Fusi Pecci, F., Ferraro, F. R., Corsi, C. E., Cacciari, C., & Buonanno, R. 1992, *AJ*, 104, 1831
- Girardi, L., Bertelli, G., Bressan, A., Chiosi, C., Groenewegen, M. A. T., Marigo, P., Salasnich, B., & Weiss, A. 2002, *A&A*, 391, 195
- Grillmair, C. J. & Smith, G. H. 2001, *AJ*, 122, 3231
- Harris, W. E. 1996, *AJ*, 112, 1487
- Hurley, J. R., Tout, C. A., Aarseth, S. J., & Pols, O. R. 2001, *MNRAS*, 323, 630
- Koch, A., Grebel, E. K., Odenkirchen, M., Martínez-Delgado, D., & Caldwell, J. A. R. 2004, [astro-ph/0408208](#)
- Landolt, A. 1992, *AJ*, 104, 340
- Leonard, P. J. T. 1996, *ApJ*, 470, 521
- Mapelli, M., Sigurdsson, S., Colpi, M., Ferraro, F. R., Possenti, A., Rood, R. T., Sills, A., & Beccari, G. 2004, *ApJ*, 605, L29
- Milone, A. A. E. & Latham, D. W. 1992, in *IAU Symp. 151, Evolutionary Processes in Interacting Binary Stars*, eds. Y. Kondo, R. F. Sistero, & R. S. Polidan, 151, 475
- Odenkirchen, M., Grebel, E. K., Dehnen, W., Rix, H.-W., & Cudworth, K. M. 2002, *AJ*, 124, 1497
- Ortolani, S., Rosino, L., & Sandage, A. 1985, *AJ*, 90, 473
- Piotto, G. et al. 2004, *ApJ*, 604, 109
- Reid, N. & Majewski, S. R. 1993, *ApJ*, 409, 635
- Romani, R. W. & Weinberg, M. D. 1991, *ApJ*, 372, 487
- Rubenstein, E. P. & Bailyn, C. D. 1997, *ApJ*, 474, 701
- Rubenstein, E. P. & Bailyn, C. D. 1999, *ApJ*, 513, L33
- Sandage, A. 1953, *AJ*, 58, 61

- Sandquist, E. L., Latham, D. W., Shetrone, M. D., & Milone, A. A. E. 2003, *AJ*, 125, 810
- Sheinis, A. I., Bolte, M., Epps, H. W., Kibrick, R. I., Miller, J. S., Radovan, M. V., Bigelow, B. C. & Sutin, B. M. 2002, *PASP*, 114, 851.
- Sandquist, E. L. & Shetrone, M. D. 2003, *AJ*, 125, 2173
- Siegel, M. H., Majewski, S. R., Cudworth, K. M., & Takamiya, M. 2001, *AJ*, 121, 935 (SMCT)
- Sigurdsson, S., Davies, M. B., & Bolte, M. 1994, *ApJ*, 431, L115
- Sills, A. & Baily, C. D. 1999, *ApJ*, 513, 428
- Sills, A., Baily, C. D., Edmonds, P. D., & Gilliland, R. L. 2000, *ApJ*, 535, 298
- Stetson, P. B. 1993, in *IAU Coll. 136, Stellar Photometry: Current Techniques and Future Developments*, ed. C. J. Butler & I. Elliot, (Cambridge: Cambridge Univ. Press), 291
- van den Berg, M., Orosz, J., Verbunt, F., & Stassun, K. 2001, *A&A*, 375, 375
- Veronesi, C., Zaggia, S., Piotto, G., Ferraro, F. R., & Bellazzini, M. 1996, in *ASP Conf. Ser. 92, Formation of the Galactic Halo...Inside and Out*, ed. H. Morrison & A. Sarajedini (San Francisco: ASP), 301
- Wilson, A. G. 1955, *PASP*, 67, 27
- Zaggia, S. R., Piotto, G., & Capaccioli, M. 1997, *A&A*, 327, 1004

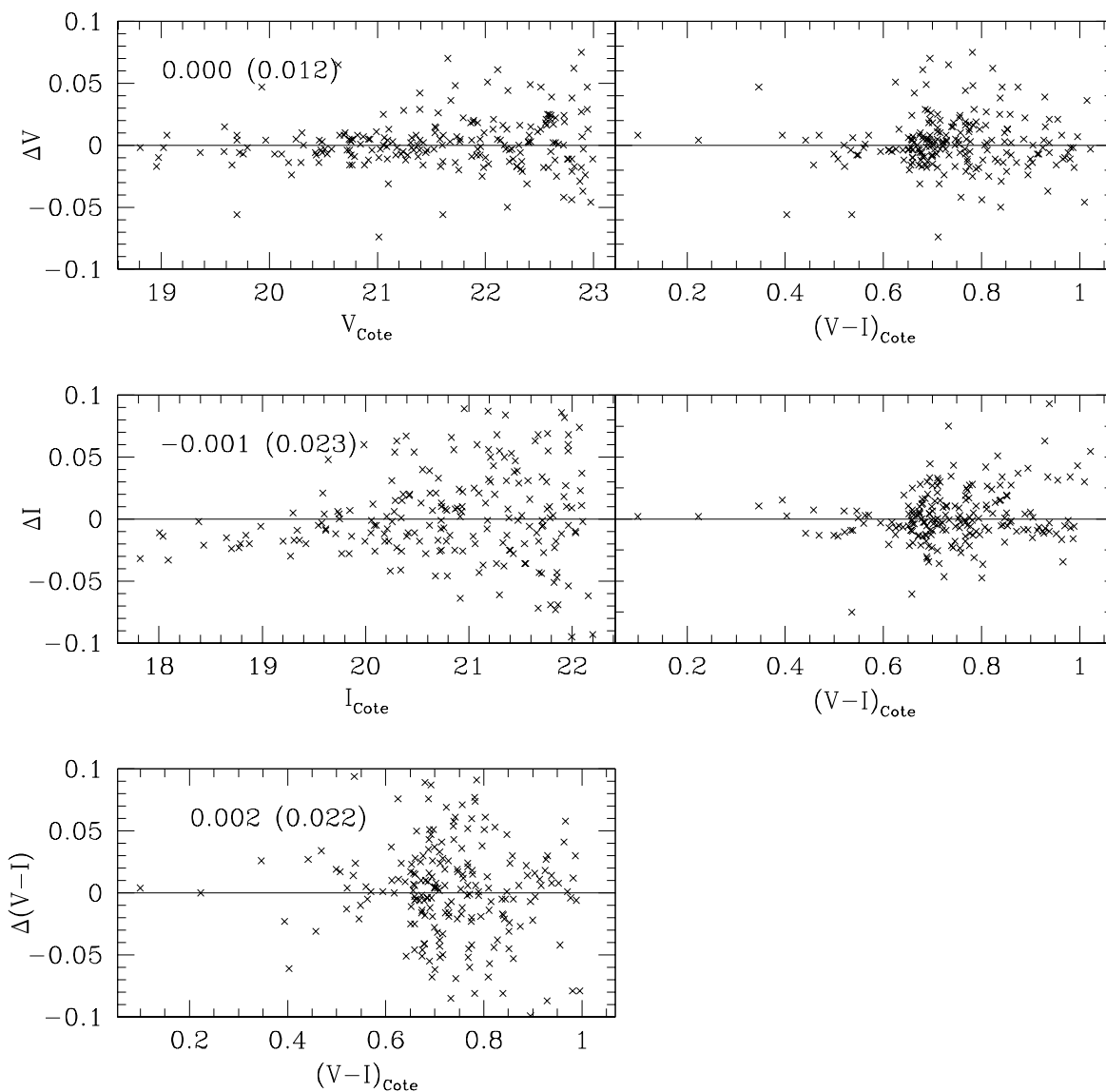


Fig. 1.— Residuals for  $V$  and  $I$  measurements of the 211 Palomar 13 stars used in our calibration (in the sense of our magnitudes minus Côté et al. (2002) magnitudes). The median residuals and semi-interquartile range (a measure of scatter) are plotted in the panels on the left.

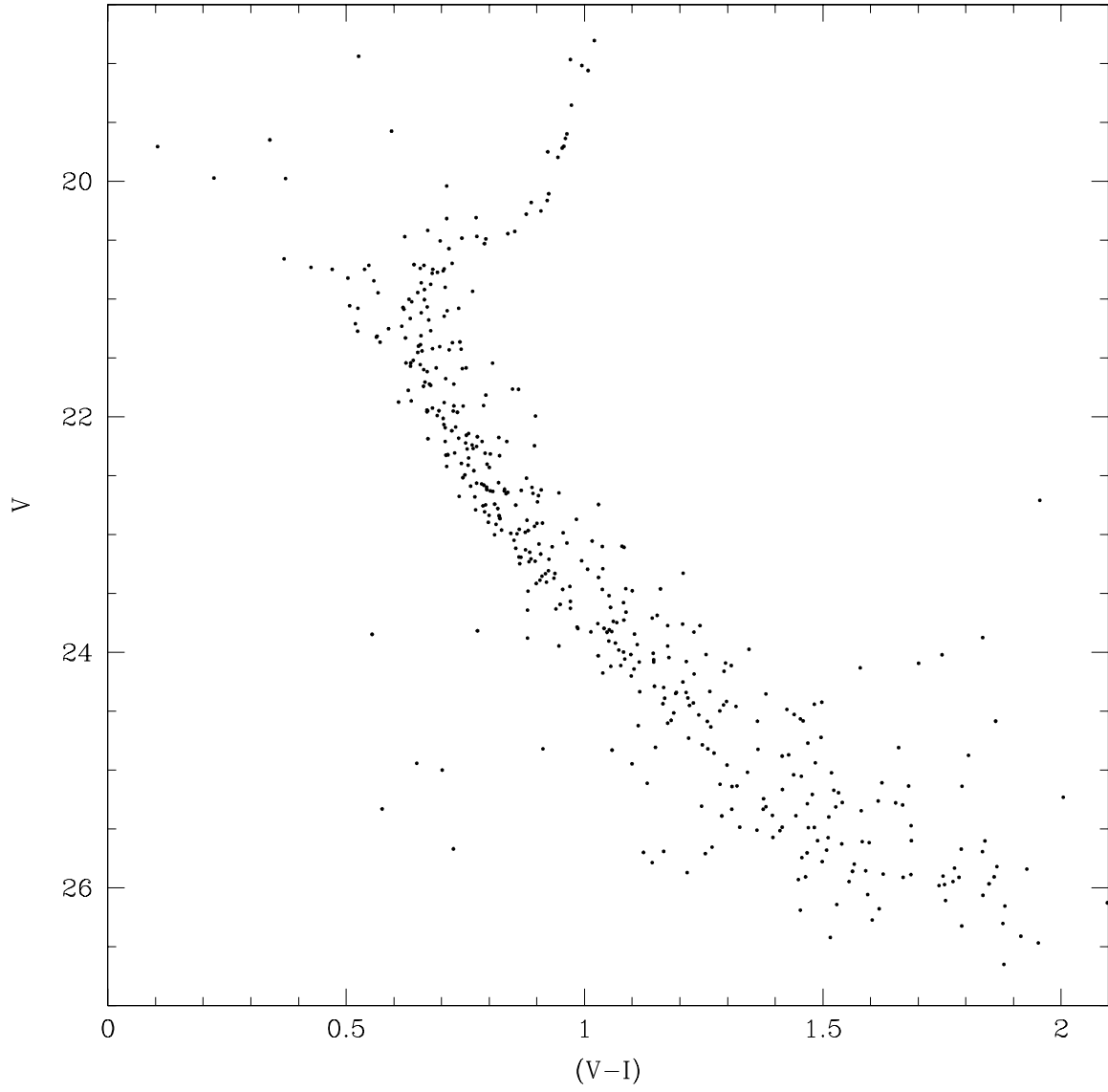


Fig. 2.— The color-magnitude diagram for Palomar 13 from our Keck photometry.

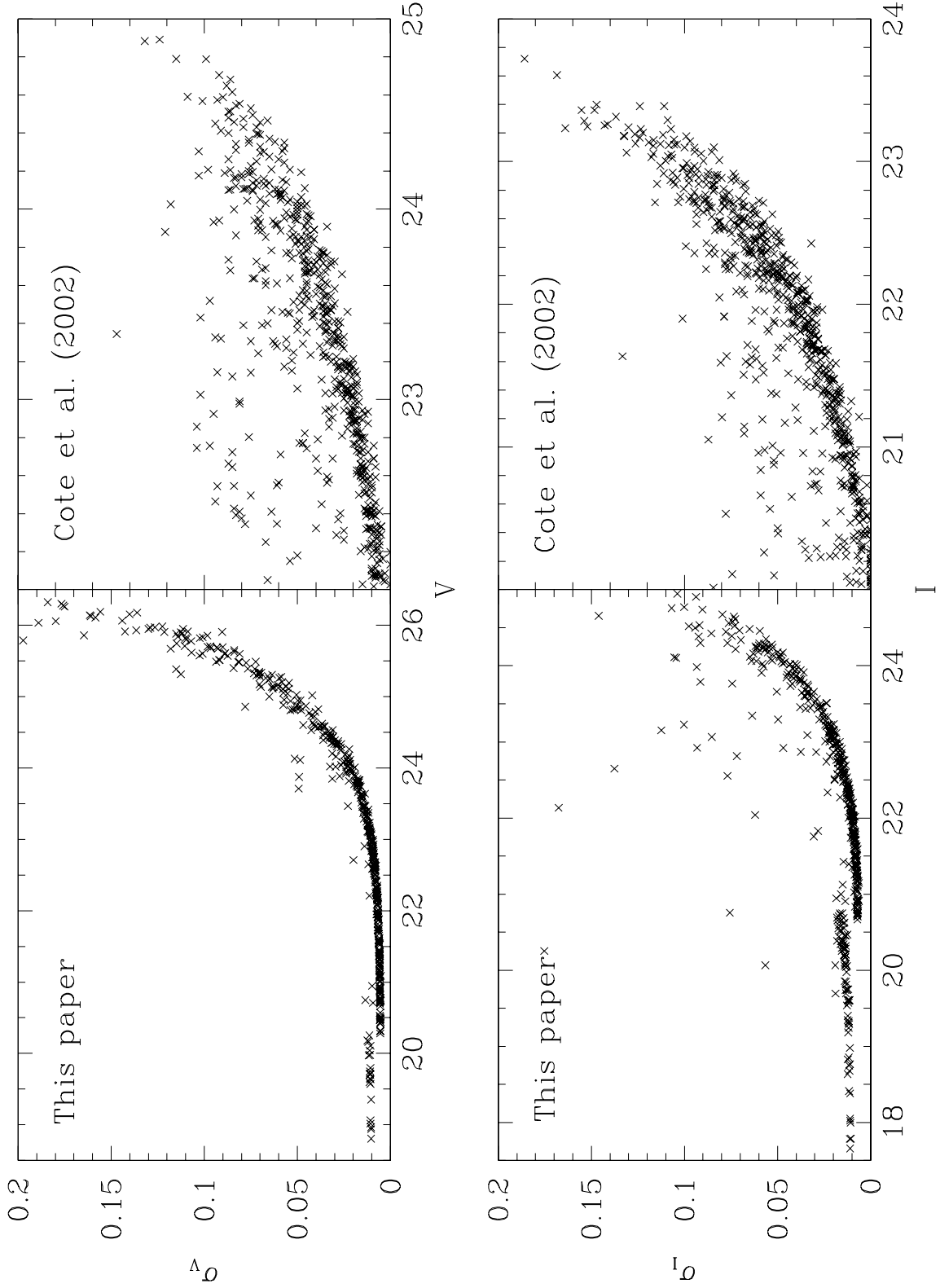


Fig. 3.— Formal measurement errors for the photometry from this study (*left panels*) and Côté et al. (2002) (*right panels*). The jumps seen at  $V \approx 20.25$  and  $I \approx 20.6$  mark the saturation limits for the long exposures in this study.

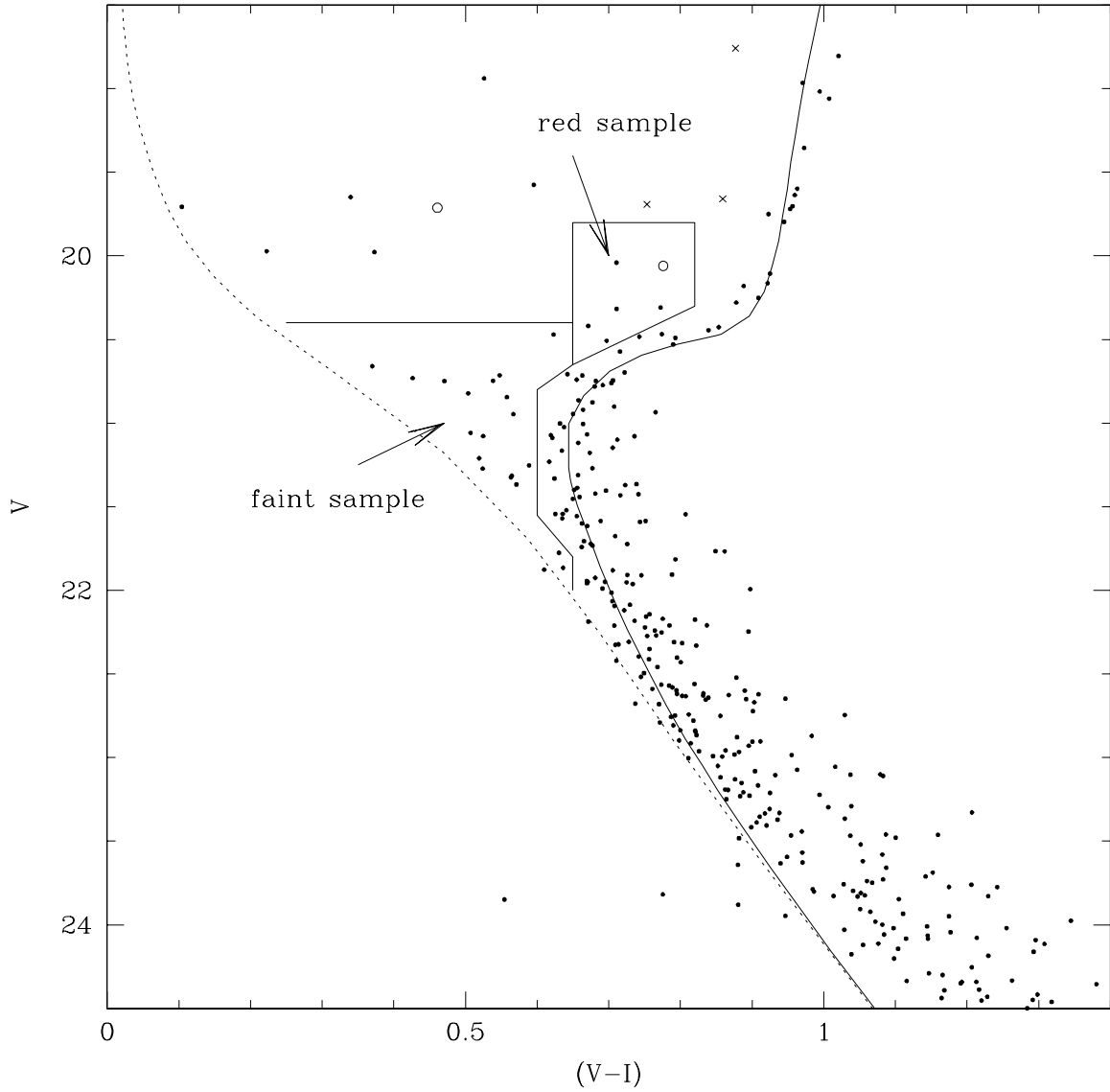


Fig. 4.— Palomar 13 blue straggler star candidates:  $\circ$  show candidates not found in our Keck field, and  $\times$  show high-probability field stars. The *solid line* shows an 11.2 Gyr isochrone and the *dashed line* shows 0.31 Gyr isochrone (Girardi et al. 2002) for  $Z = 0.0004$ ,  $E(V - I) = 0.13$ , and  $(m - M)_V = 17.37$

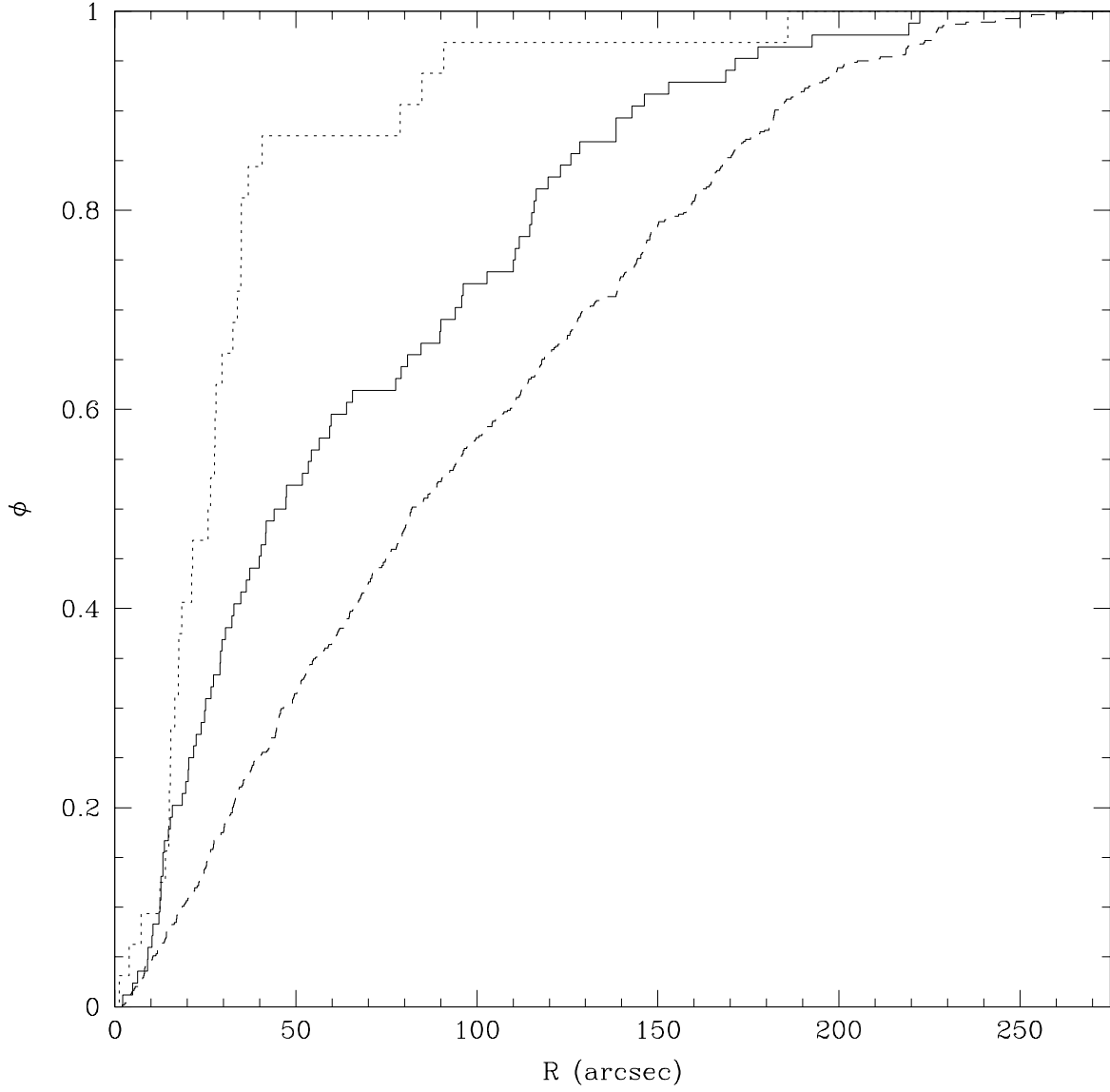


Fig. 5.— Normalized cumulative radial distributions for giant and subgiant stars (*solid line*), main sequence stars (*dashed line*), and blue stragglers (*dotted line*).



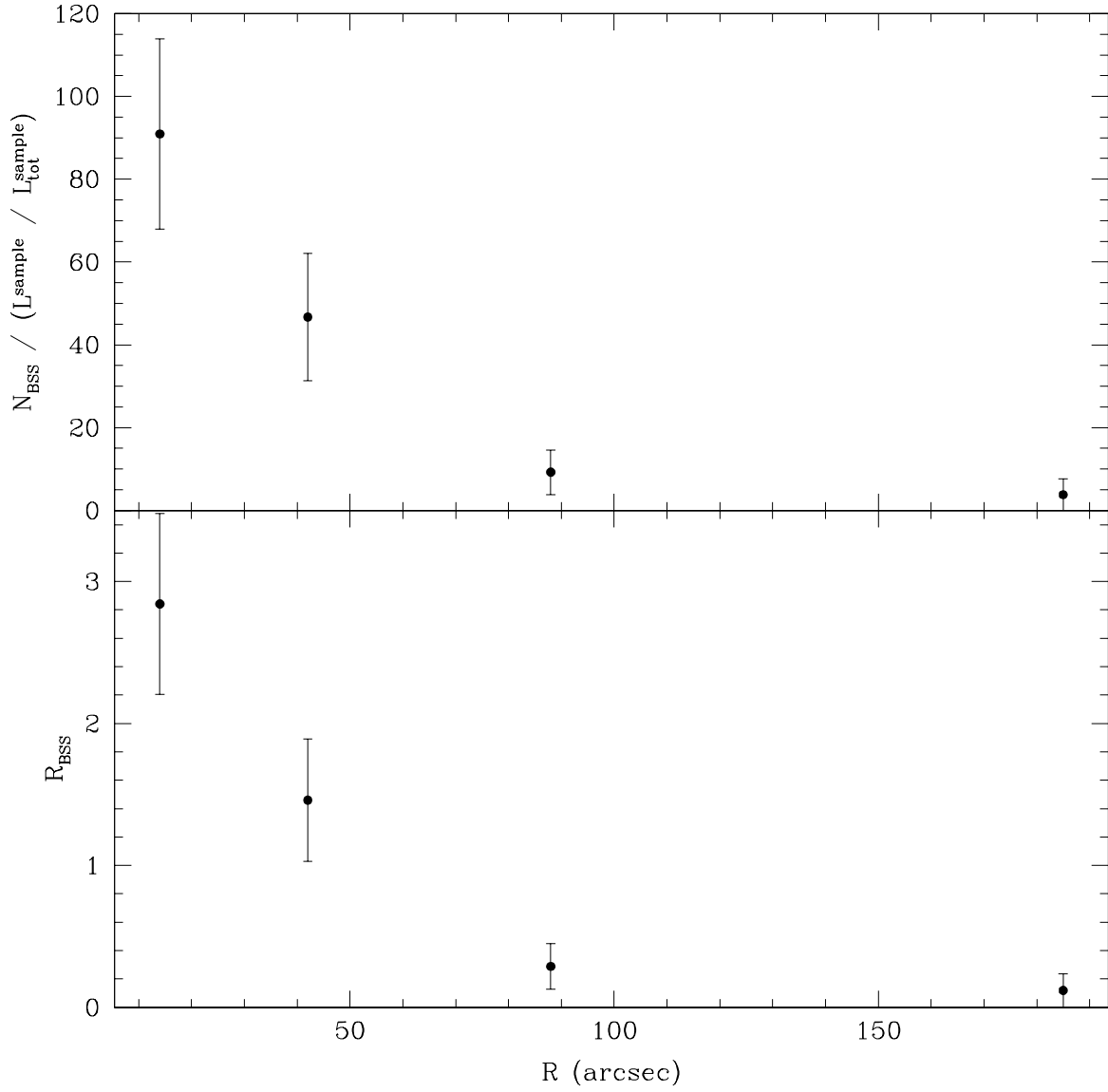


Fig. 6.— *Top panel:* Frequency of blue stragglers relative to the integrated  $V$ -band flux of detected cluster stars. *Bottom panel:* specific frequency of blue stragglers relative to the integrated flux.

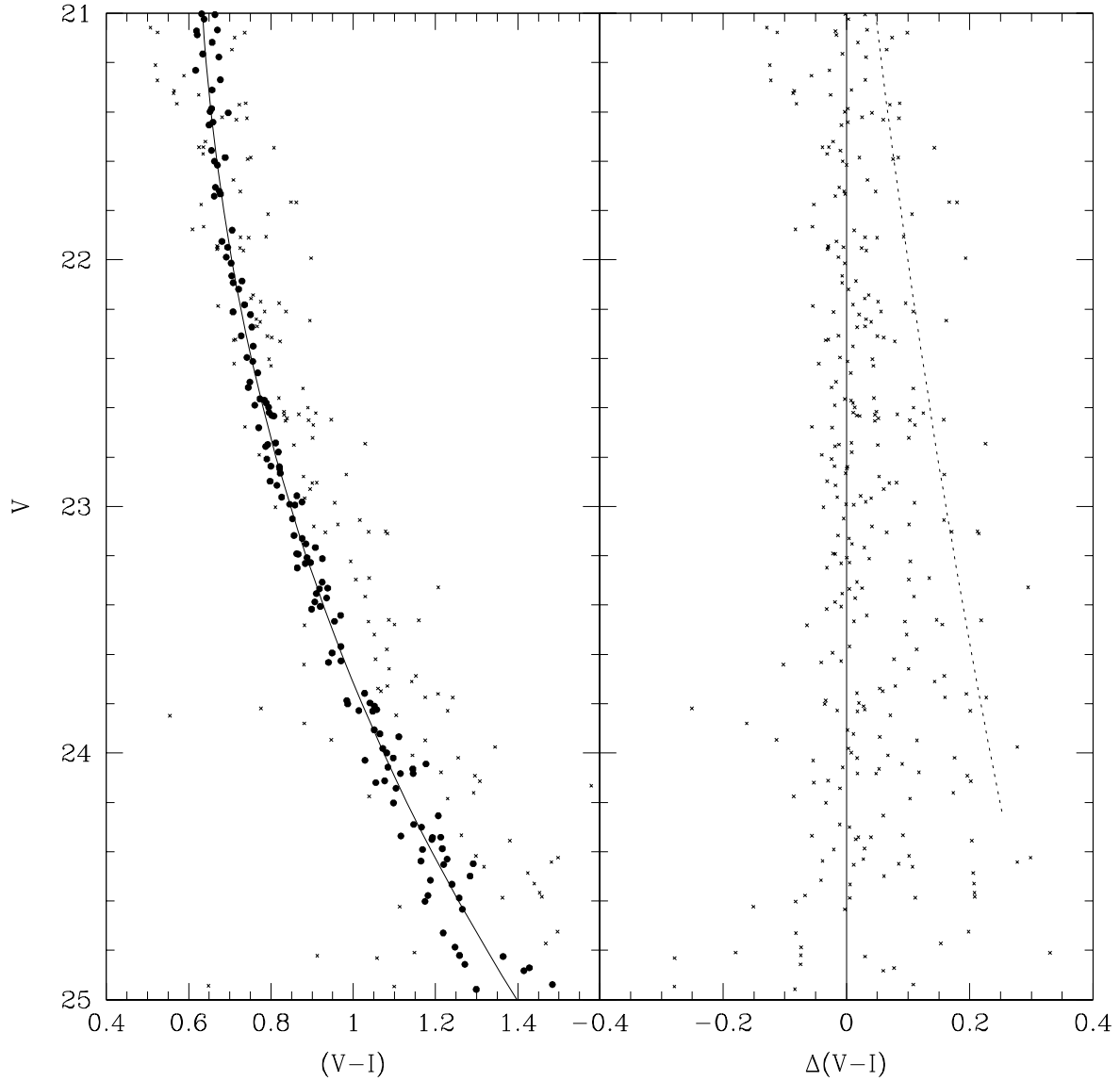


Fig. 7.— *Left panel:* The Palomar 13 main sequence CMD. The *solid line* is the polynomial fit to the main sequence stars shown with  $\bullet$ . These stars have photometric errors placing them less than  $2.5\sigma$  from the polynomial fit. *Right panel:* The rectified CMD (with the color of the polynomial fit subtracted from the color of each star). The *dotted line* shows the expected positions for equal-mass binaries.

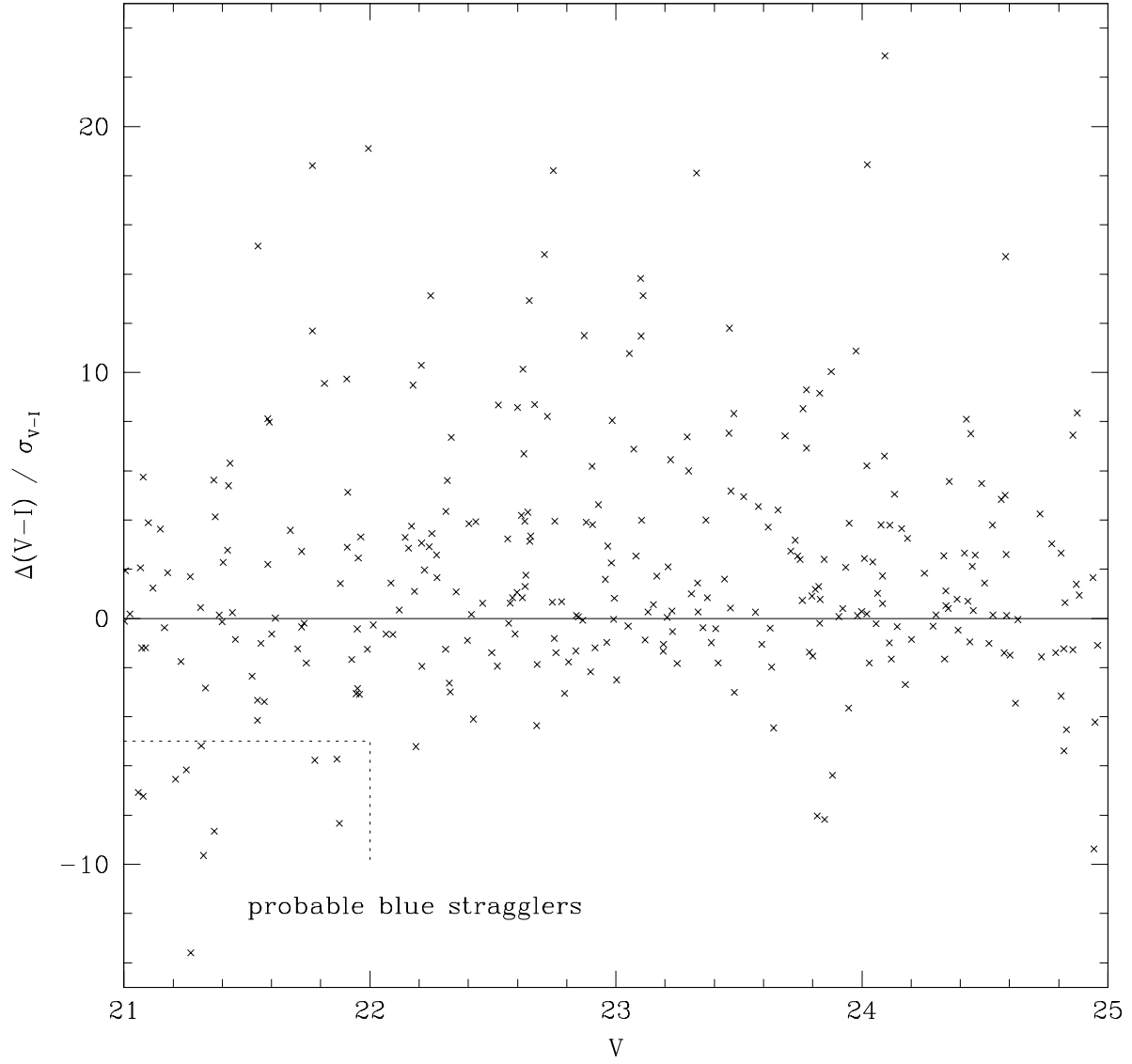


Fig. 8.— The significance of color deviations  $\Delta(V - I)/\sigma_{V-I}$  versus magnitude for Palomar 13 stars. Positive  $\Delta(V - I)$  indicates that the star is to the red of the main sequence fit.

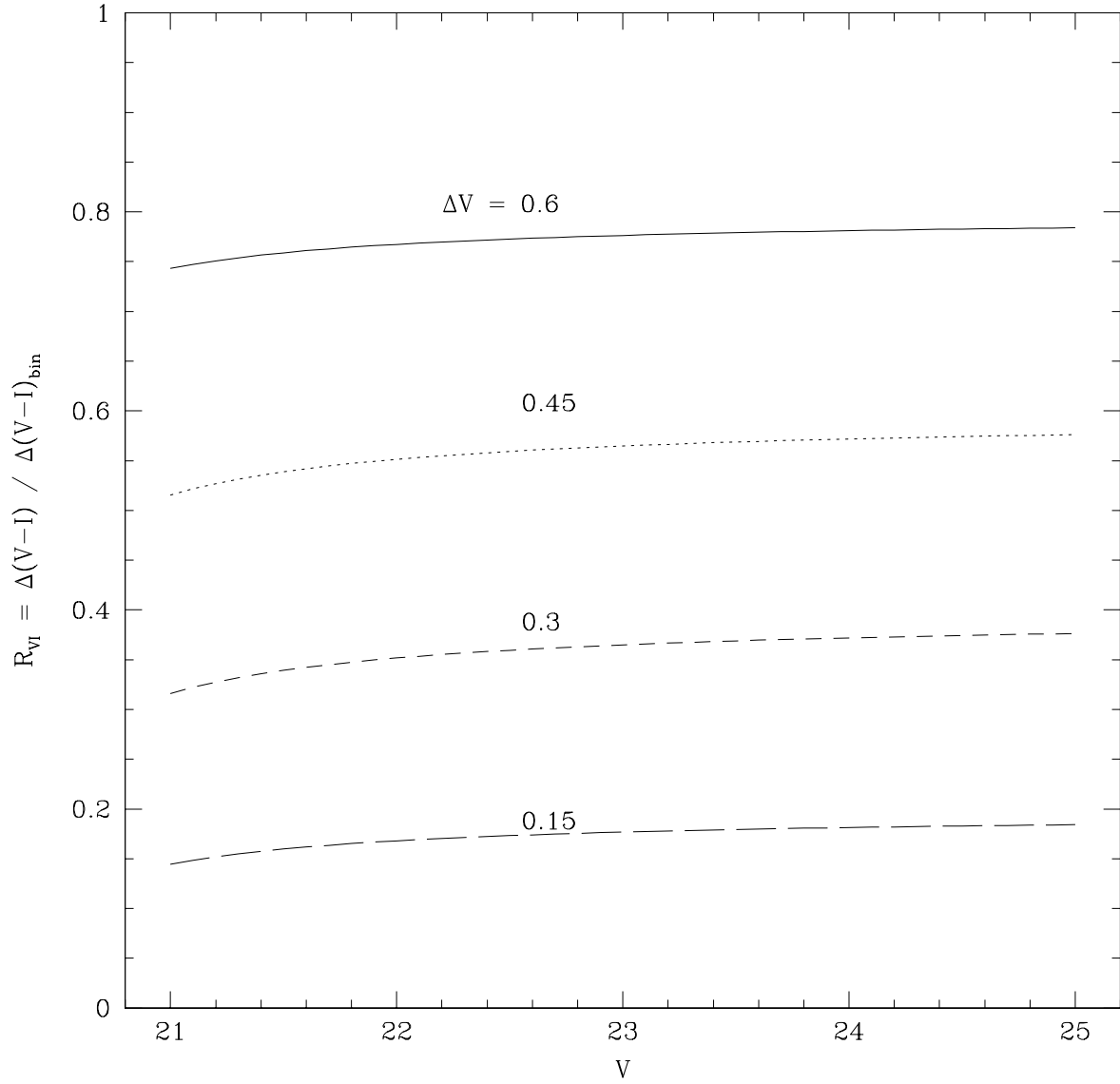


Fig. 9.— The relationship between  $R_{VI} = \Delta(V-I)/\Delta(V-I)_{bin}$  and the  $\Delta V$  (the magnitude change to a star’s measured magnitude due to the addition of the light of an unresolved star).

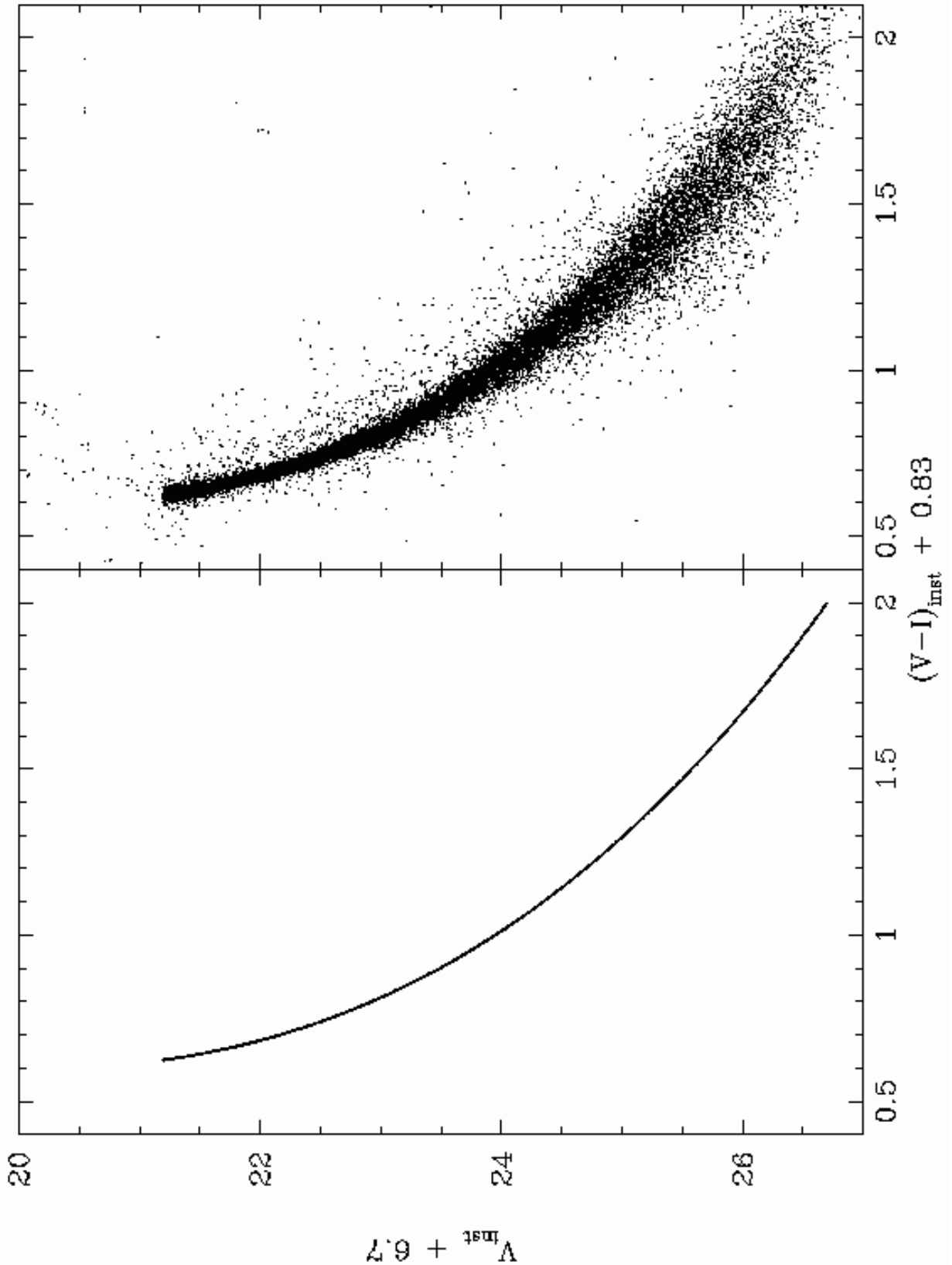


Fig. 10.— Color-magnitude diagrams of artificial star experiments on the Keck ESI data. The instrumental magnitude and color have been adjusted to roughly overlie the calibrated data. *Left panel:* Input artificial stars. *Right panel:* Photometry of objects detected at the positions of the input artificial stars.

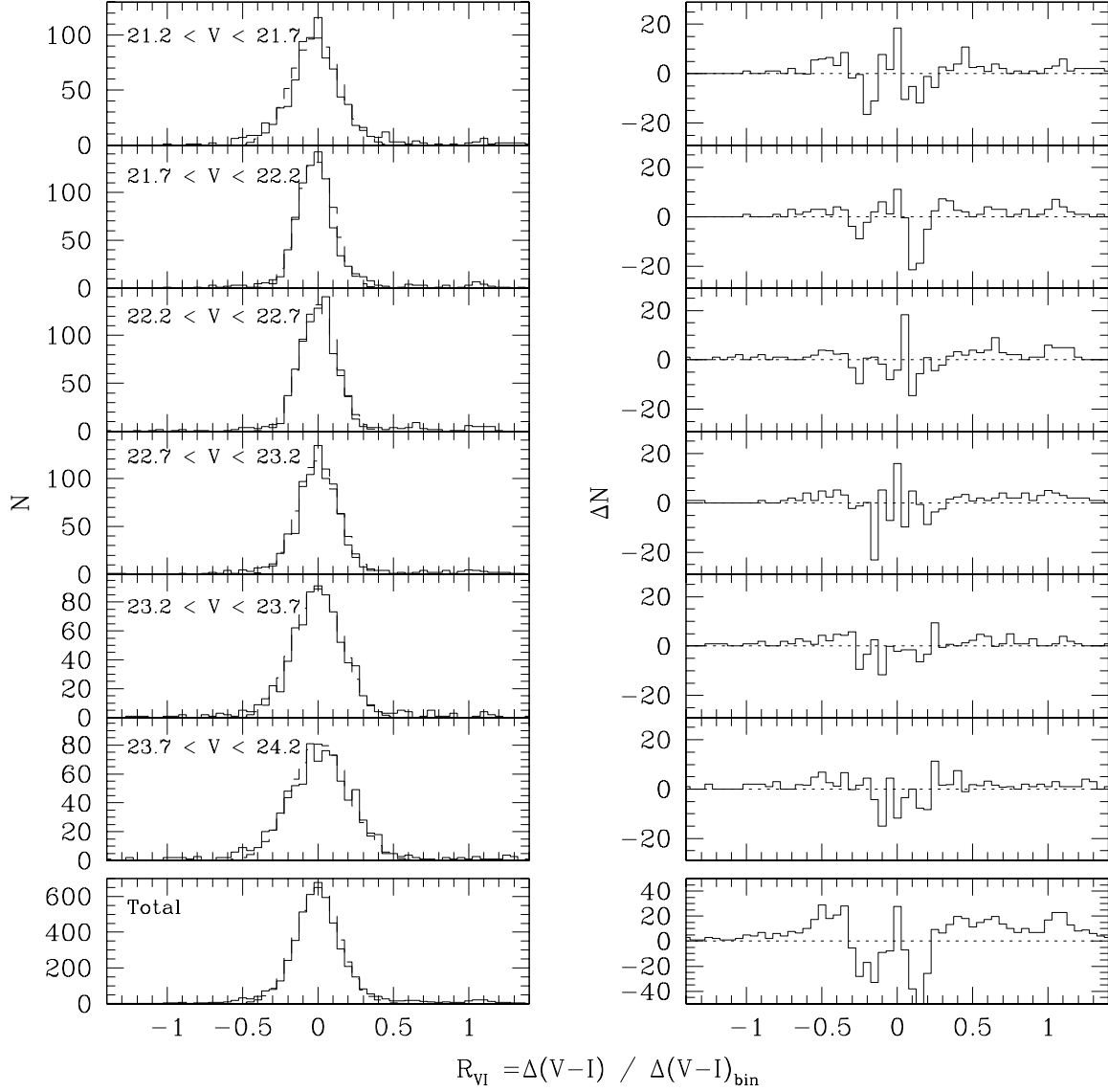


Fig. 11.— *Left panels*: Normalized color deviations  $R_{VI}$  for artificial stars within  $1'$  of the center of the cluster, separated by magnitude. A Gaussian fit (*dashed line*) to the distribution is shown in the top 6 panels, while the sum of these fits is shown in the “Total” panel. *Right panels*: The residuals after the fits are subtracted from the distributions.

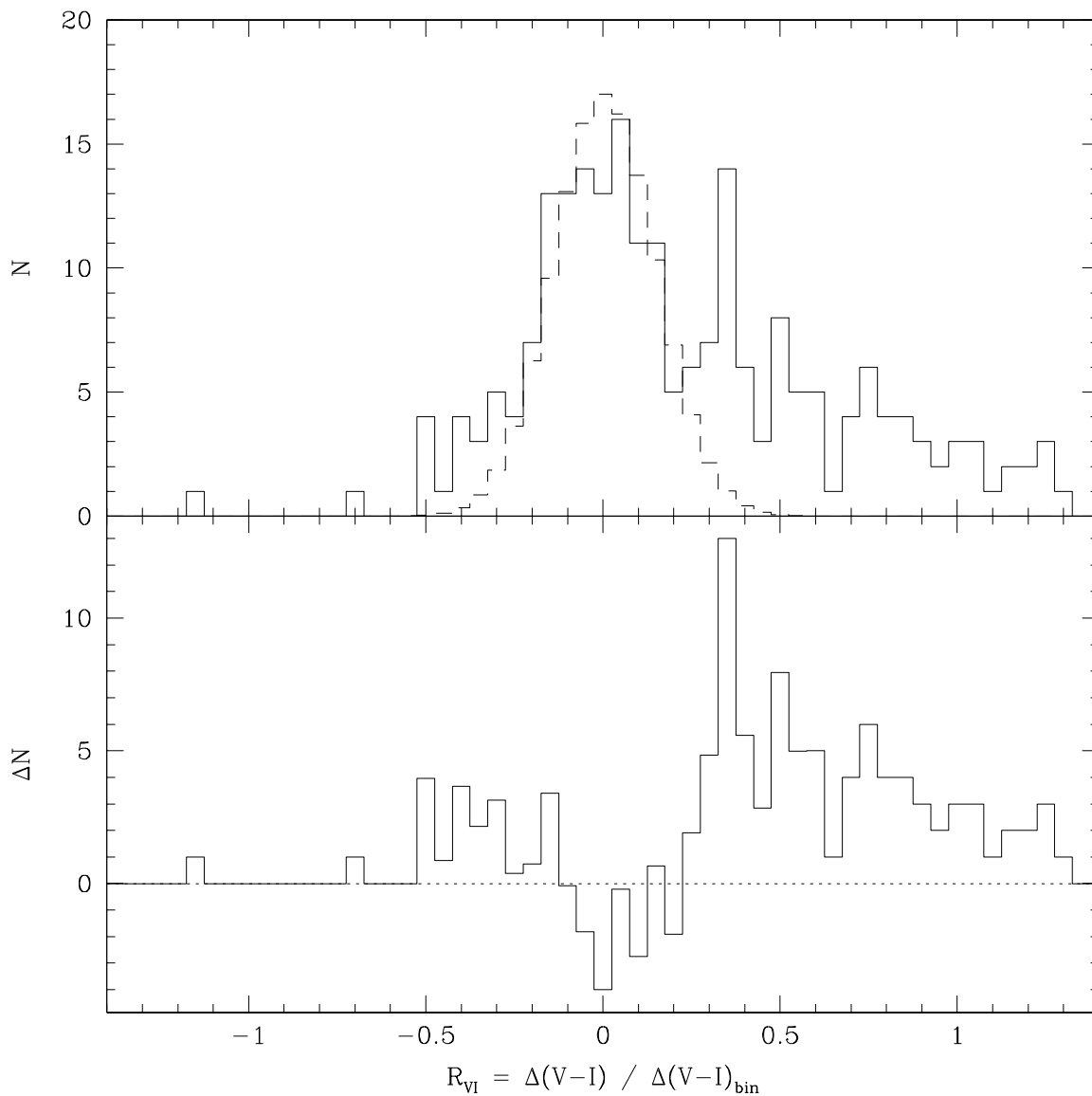


Fig. 12.— *Top panel:* The distribution of color deviations (star color minus the color of single star sequence at the same  $V$  magnitude) relative to the color difference between the single star sequence and equal-mass binary sequence for Palomar 13 main sequence stars. The *dashed line* shows the Gaussian fit to stars with  $|\Delta(V - I)/\Delta(V - I)_{bin}| < 0.3$ . *Bottom panel:* The subtraction of the Gaussian fit from the star distribution.

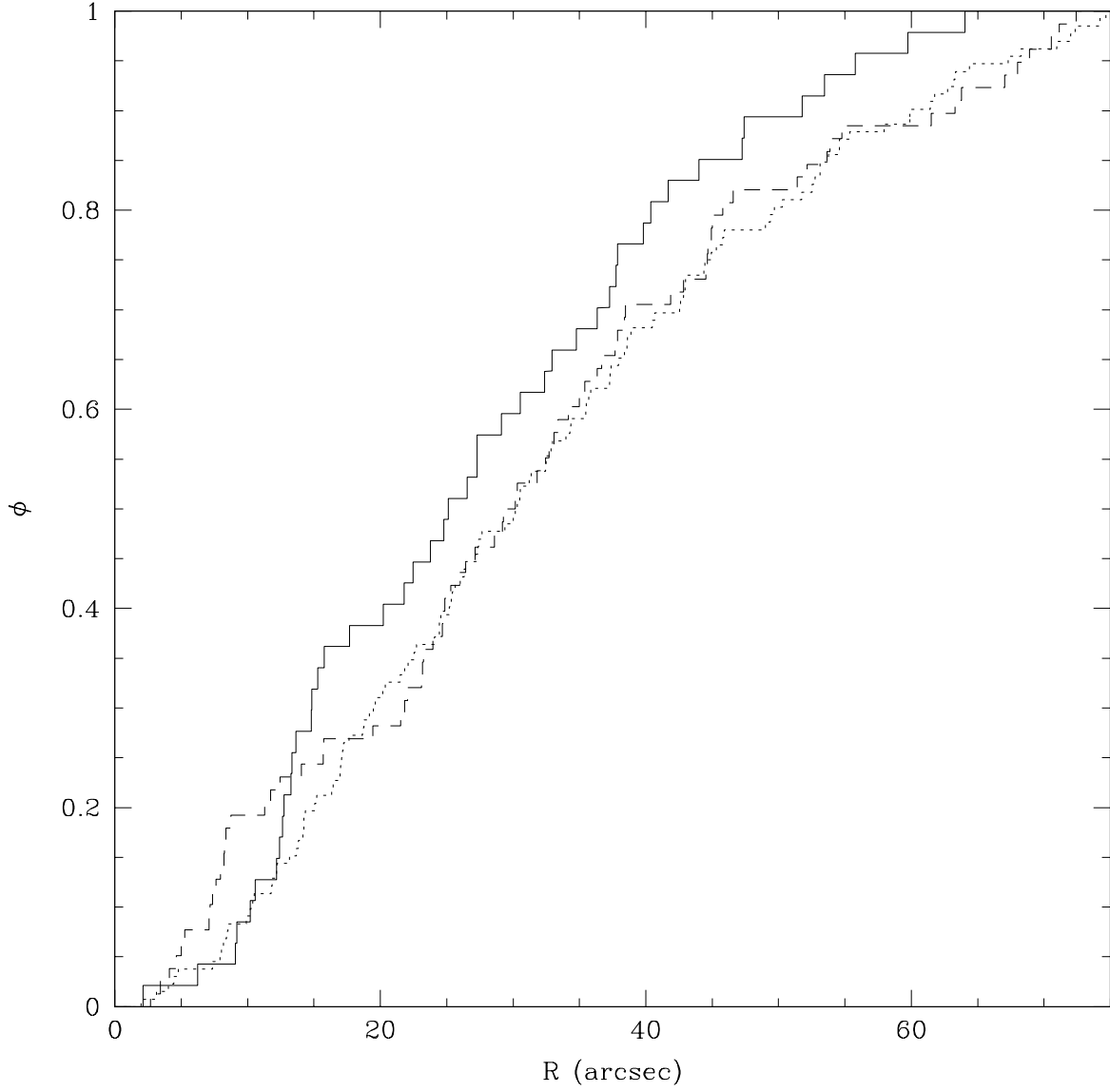


Fig. 13.— Normalized cumulative radial distributions for giant and subgiant stars (*solid line*), probable single main sequence stars (*dashed line*), and probable main sequence binary systems (*dotted line*).



Table 1. Straggler Star Candidates

ID	SMCT	CDMCM <sup>1</sup>	$\Delta\alpha$ (")	$\Delta\delta$ (")	$V$	$(V - I)$	$(B - V)$	$(U - V)$	$P$	Notes
2 <sup>2</sup>	79	29	−7.38	−28.60	18.939 ± 0.010	0.526 ± 0.016				rv member
					18.956	0.521	0.373			
7 <sup>2</sup>	125	38	−11.05	−30.67	19.021					
					19.575 ± 0.011	0.595 ± 0.015		0.397	0.65	BSS 9 (SMCT)
					19.580	0.594	0.463			
9 <sup>23</sup>	126	40	21.70	−27.35	19.603					
					19.649 ± 0.011	0.340 ± 0.016		0.463	0.58	BSS 8 (SMCT)
					19.700	0.403	0.455	0.463	0.95	BSS 6 (SMCT)
11 <sup>23</sup>	124	41	−0.52	1.07	19.714					
					19.707 ± 0.011	0.104 ± 0.016		0.341	0.95	BSS 6 (SMCT)
					19.699	0.100	0.161			
16 <sup>23</sup>	167	55	−9.42	12.08	19.687					
					19.712	0.461	0.190	0.322	0.80	BSS 5 (SMCT)
					19.741	0.387	0.389	0.461	0.79	BSS 7 (SMCT)
17 <sup>23</sup>	179	52	−20.09	28.56	19.972 ± 0.011	0.223 ± 0.017				
					19.968	0.223	0.214			
					20.001		0.210	0.294	0.75	BSS 2 (SMCT)
29	239	79	−26.38	−0.35	19.977 ± 0.011	0.373 ± 0.017				
					19.932	0.346	0.295			
					19.991		0.264	0.329	0.81	BSS 1 (SMCT)
36	289	99	−27.13	−74.02	20.471 ± 0.006	0.623 ± 0.014				binary or BSS?
					20.475	0.612	0.520			
					20.374		0.427	0.347	0.97	
40 <sup>23</sup>	306	98	−6.25	15.36	20.660 ± 0.005	0.370 ± 0.015				
					20.650	0.394	0.337			
					20.680		0.331	0.252	0.98	
42	356	100	31.22	−13.09	20.715 ± 0.006	0.548 ± 0.015				
					20.720	0.534	0.426			
					20.760		0.397	0.069	0.87	BSS 3 (SMCT)
43	352	108	2.87	−27.79	20.731 ± 0.006	0.426 ± 0.016				
					20.744	0.458	0.342			
					20.851		0.373	0.269	0.91	
45	366	110	13.09	−22.18	20.749 ± 0.006	0.471 ± 0.015				member?
					20.746	0.442	0.374			
					20.885		0.326	0.154	0.49	
52	364	118	3.28	−12.00	20.747 ± 0.006	0.539 ± 0.015				
					20.755	0.549	0.417			
					20.793		0.460	0.418	0.46	
53	497	148	−20.51	5.12	20.822 ± 0.006	0.504 ± 0.015				unresolved blend in SMC
					20.817	0.469	0.382			
					20.845 ± 0.006	0.558 ± 0.015				
64	497	148	−35.63	19.66	20.843	0.563	0.457			
					20.827		0.384	0.480	0.57	
					21.058 ± 0.006	0.507 ± 0.018				
					21.057	0.520	0.396			
					21.058		0.434	0.553	0.86	

Table 1—Continued

ID	SMCT	CDMCM <sup>1</sup>	$\Delta\alpha$ (")	$\Delta\delta$ (")	$V$	$(V - I)$	$(B - V)$	$(U - V)$	$P$	Notes
67	504	158	−31.85	−18.55	$21.078 \pm 0.006$	$0.525 \pm 0.016$				field?
					21.090	0.507	0.433			
					21.104		0.371	0.207	0.07	
75	524	167	−10.24	−11.64	$21.210 \pm 0.006$	$0.519 \pm 0.019$				
					21.218	0.499	0.402			
					21.132		0.468	0.339	...	
77	623	180	−25.92	9.65	$21.253 \pm 0.006$	$0.589 \pm 0.009$				
					21.262	0.642	0.486			
					21.249		0.515	0.577	0.59	turnoff star?
78	598	172	−6.49	2.99	$21.272 \pm 0.006$	$0.524 \pm 0.009$				
					21.279	0.546	0.436			
					21.310		0.476	0.099	0.85	
80	693	183	−12.35	−12.62	$21.315 \pm 0.006$	$0.565 \pm 0.016$				
					21.317	0.560	0.464			
					21.389		0.506	0.239	...	
82	721	182	15.82	−7.48	$21.324 \pm 0.006$	$0.563 \pm 0.009$				member?
					21.319	0.538	0.441			
					21.362		0.596	0.249	0.51	
84	461	190	2.37	−3.17	$21.367 \pm 0.006$	$0.571 \pm 0.009$				
					21.358	0.570	0.433			
					21.080		0.433	0.148	...	
112	1041	255	26.59	−80.51	$21.776 \pm 0.007$	$0.631 \pm 0.009$				
					21.768	0.689	0.484			
					21.773		0.463	0.215	0.53	
116		275	−8.74	19.62	$21.867 \pm 0.007$	$0.636 \pm 0.010$				
117	1169	279	−13.25	−7.20	21.872	0.679		0.523		
					$21.877 \pm 0.007$	$0.610 \pm 0.010$				
					21.871	0.659	0.522			
					22.043		0.358	−0.134	0.17	
Stars Redder than Turnoff										
18	202	58	33.56	9.54	$20.041 \pm 0.011$	$0.711 \pm 0.016$				binary?
					20.048	0.709	0.520			
					20.038		0.620	0.547	0.85	
24	214	61	−24.19	−87.54	20.060	0.776		0.590		binary?; outside field
					20.121		0.590	0.497	0.99	
					$20.309 \pm 0.006$	$0.772 \pm 0.014$				unresolved blend in SMC?
25	218	70	−13.88	1.08	20.300	0.757		0.593		
					$20.317 \pm 0.005$	$0.711 \pm 0.013$				prob. binary
					20.317	0.702	0.529			
26	274	75	26.88	−6.22	$20.243$			0.504	0.301	0.94
					$20.419 \pm 0.006$	$0.671 \pm 0.014$				prob. binary
					20.425	0.678	0.532			
33	301	86	−14.45	−3.34	20.413			0.604	0.541	0.91
					$20.508 \pm 0.006$	$0.697 \pm 0.014$				prob. binary
					20.512	0.671	0.532			
					20.608		0.434	0.310	0.90	

Table 1—Continued

ID	SMCT	CDMCM <sup>1</sup>	$\Delta\alpha$ (")	$\Delta\delta$ (")	$V$	$(V - I)$	$(B - V)$	$(U - V)$	$P$	Notes
Probable Red Giant Binary Stars										
3	88	30	-14.44	-41.58	$18.966 \pm 0.010$	$0.971 \pm 0.015$				
					18.976	0.970	0.749			
					18.970		0.757	0.872	0.93	
14	182	49	3.06	-21.59	$19.751 \pm 0.011$	$0.923 \pm 0.016$				
					19.758	0.917	0.716			
					19.795		0.644	0.592	0.98	
High-Probability Field Stars										
	76	26	-12.51	-92.52	18.758	0.877	0.744			rv nonmember; outside fi
					18.743		0.777	1.018	0.00	
	154	45	68.75	-116.52	19.692	0.753	0.547			outside field
					19.715		0.584	0.529	0.00	
	168	43	-178.63	-134.63	19.659	0.859	0.706			outside field
					19.704		0.594	0.511	0.00	

<sup>1</sup>Côté et al. (2002).

<sup>2</sup>Blue straggler star candidate from Siegel et al. (2001; SMCT).

<sup>3</sup>Blue straggler star candidate from Borissova et al.(1997; BMS).

Table 2. K-S Test Results for Radial Distribution Comparisons

Sample 1	Sample 2	$D$	$P$
Côté et al. (2002) Samples			
BSS	GB	0.42	0.00042
BSS	MS	0.62	$5 \times 10^{-11}$
GB	MS	0.23	0.00060
BSS $[(V - I) < (V - I)_{TO}]$	GB	0.42	0.0011
BSS $[(V - I) < (V - I)_{TO}]$	MS	0.63	$2 \times 10^{-9}$
BSS $[V > 20.4]$	GB	0.43	0.0041
BSS $[V > 20.4]$	MS	0.64	$2 \times 10^{-7}$
BSS $[V < 20]$	GB	0.44	0.12
BSS $[V < 20]$	MS	0.63	0.0036
ESI Field Samples			
Binaries	MS	0.11	0.55
RGB	MS+Binaries	0.13	0.51

Table 3. Keck ESI Photometry of Palomar 13

ID	$\Delta\alpha''$	$\Delta\delta''$	$X$ (pix)	$Y$ (pix)	$V$	$\sigma_V$	$I$	$\sigma_I$
1	−2.09	12.00	284.92	514.71	18.805	0.010	17.784	0.011
2	−7.38	−28.61	286.72	780.19	18.939	0.010	18.413	0.012
3	−14.43	−41.58	321.84	868.99	18.966	0.010	17.996	0.011
4	−5.35	−7.49	290.46	642.66	19.017	0.011	18.023	0.011
5	0.86	12.71	266.54	507.95	19.060	0.011	18.052	0.011
6	−32.40	40.37	502.77	354.47	19.355	0.010	18.382	0.011
7	−11.05	−30.67	308.69	796.20	19.575	0.011	18.980	0.011
8	−12.17	2.39	342.20	584.09	19.598	0.011	18.635	0.012
9	21.70	−27.35	100.45	750.53	19.649	0.011	19.309	0.012
10	11.46	−38.14	157.82	827.63	19.636	0.011	18.677	0.011
11	−0.52	1.07	266.15	583.94	19.707	0.011	19.602	0.012
12	−20.27	−9.65	384.82	667.65	19.703	0.011	18.747	0.012
13	12.57	4.24	184.34	553.86	19.719	0.011	18.766	0.011
14	3.06	−21.59	225.04	727.25	19.750	0.011	18.828	0.012

Note. — The complete version of this table is in the electronic edition of the Journal. The printed edition contains only a sample.